MITIGATION OF OZONE PRODUCTION BY NEGATIVE CORONA USING ELECTRODE WIRE HEATING

by

Nicholas August Meyer

Thesis submitted to the Faculty of the
Virginia Polytechnic Institute and State University
in partial fulfillment of the requirements for the degree of

MASTER OF SCIENCE

in

Environmental Engineering

APPROVED:

Dr. J. M. Hughes, Chairman

Dr. G. D. Boardman

Dr. A. M. Dietrich

January, 1993

Blacksburg, Virginia

c.2

MITIGATION OF OZONE PRODUCTION BY NEGATIVE CORONA USING ELECTRODE WIRE HEATING

by

Nicholas August Meyer

Committee Chairman: J. Martin Hughes
Environmental Engineering

(ABSTRACT)

Ozone generation is a problem associated with indoor air cleaners that utilize a corona to ionize particles. This experimentation utilized a negative corona and investigated the effect that external electrode wire heating had on the ozone production rate. Results showed that the ozone generation rate could be significantly reduced by raising the electrode surface temperature to 85 ^{o}C. Above this temperature, no further ozone reduction was observed.

A linear relationship existed between ozone concentration and corona current. A parabolic relationship existed between corona current and corona voltage potential. Smaller corona wire diameters produced ozone at lower rates than larger corona wire diameters.

A description of the investigation, the data collected, and a discussion of all results is included.

Acknowledgements

The author would like to Dr. J. Martin Hughes for the time devoted in the classroom, laboratory, and in his office toward the attainment of the author's Master's Degree. Special thanks is given to Dr. Hughes for helping prepare this document and setting aside money for use during times when research dollars were hard to find. Appreciation is also given to Dr. Andrea M. Dietrich and Dr. Gregory D. Boardman for their time in the classroom and serving on the author's committee.

The author also is grateful to Liu Linmao, who thought of the basic concepts that this work is based on, and the author hopes that his patent application will be reviewed favorably.

Gratitude for help assembling the test apparatus is given to Julie Petruska and Clarke Brown, who constantly helped a confused graduate student through the rough beginnings of this project.

Finally, the author is thankful for the constant support of his family and friends throughout his lifetime and hopes that he has been just as supportive to them. Special thanks to my father who gave me the computer that this document was composed on. Without this machine, the road to a Master's Degree would have been a little rockier.

TABLE OF CONTENTS

LIST OF FIGURES

LIST OF TABLES

I. Introduction

This research examined the hypothesis that operating conditions for a negative corona can be identified which minimize ozone production while maximizing negative ion density. The results will provide information for use in development of a more effective indoor air cleaner. At the present time, most indoor air cleaners use a positive corona to produce ions that in turn collect particulate matter. Positive corona discharges produce less ozone than negative corona discharges[1]. However, this method produces fewer ions because positive coronas spark at lower voltages (arc sooner) and produce a lower corona current for a given voltage than negative corona discharges.

Indoor air cleaners, IAC's, must operate with reduced voltages in order to comply with the Food and Drug Administration (FDA) ozone concentration requirements. The FDA regulation stipulates that the ozone level generated by an indoor air cleaner must be less than 50 ppb (0.05 ppm)[2]. Reduced voltage operation reduces ozone generation rates. At these lower voltages, less current is discharged and fewer ions are produced which lowers collection efficiencies. The plan in this investigation was to use higher negative voltages to generate higher ion concentrations (increase in

collection efficiency) without excessive ozone emissions. Heated corona discharge wires were the technique used to counteract the formation of ozone.

Awad and Castle[3] and later Ohkubo *et al.*[4] used heated wires in electrostatic precipitators (ESP) to reduce ozone emissions using both positive and negative coronas. The results did not directly apply to this study because the corona wire configuration used in ESP's differed from the one used in this research as seen in Figure 1. Note that in a plate type ESP, the air flows parallel to the grounded collecting plates and perpendicular to the discharge wires. In this study, all wires were oriented perpendicularly to the air flow as seen in Figure 1. This orientation conformed to the need for the grounded screen wires to be incorporated into the filter media of the IAC. The wires formed a pattern similar to that of jail bars.

The research investigated the following relationships. The relationship between corona current and corona voltage and the effect of electrical resistance heating, used to increase the wire temperature, on the relationship were examined. Awad and Castle[3] showed that the onset voltage was lower with wire heating. Ozone emissions and current, also as a function of wire heating, were studied. Awad and Castle[3] reported that ozone production increased with an increase in current. The increase can be offset by wire heating to some extent. Ozone concentration reductions

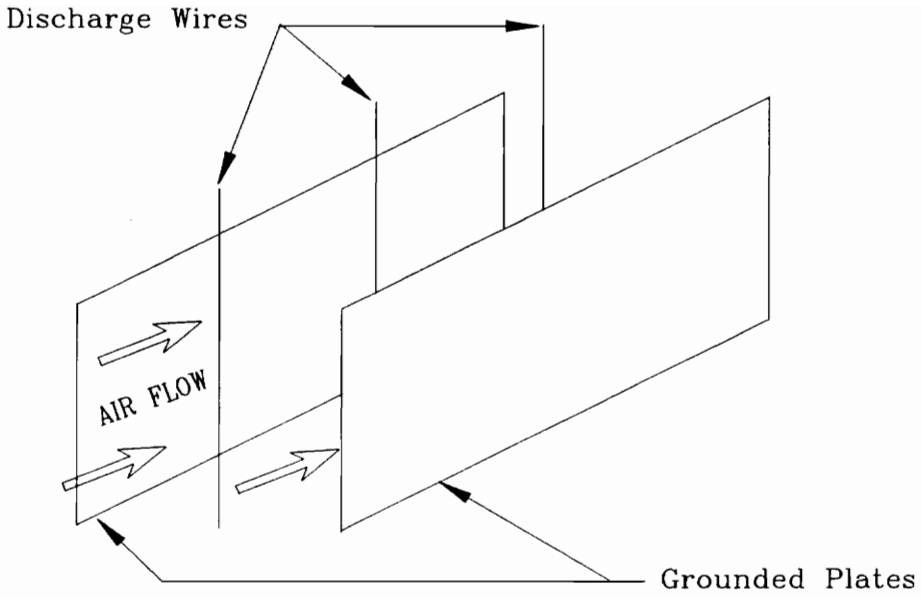

A) Typical ESP Geometry

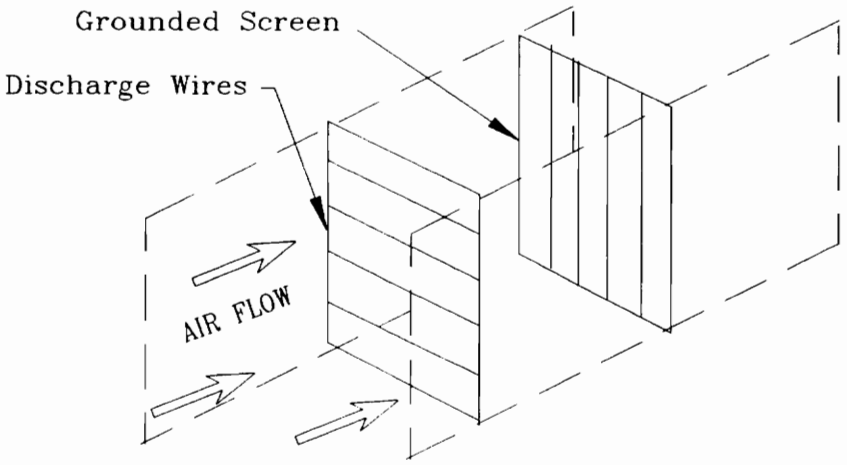

B) Wire-Screen Geometry

Figure 1. Geometrical differences between A) an ESP and B) Wire-screen setup researched

achieved by increases in the wire temperature appear to be limited to a peak wire temperature. The limit, using Ohkubo *et al.*'s[4] data and the relevant heat transfer equations, was 100 °C. Therefore, this research focused on wire temperatures in the 40 to 100 °C range.

The investigation used four wire sizes in the range of 0.1 to 0.3 millimeters (mm). Different wire diameters, when operated in the corona discharge mode, produce ozone at different rates. Previously, Castle *et al.*[5] showed that a positive corona applied in a cylindrical type ESP increased ozone production as the wire size was increased. Therefore, the ideal wire size would be expected to be the smallest diameter wire with the necessary mechanical strength to prevent breakage[3].

Utilizing the present database of knowledge outlined earlier in this section, the following objectives were chosen for this research.

(1) To relate the applied voltage potential associated with a negative corona to the corona current

(2) To determine the effect of wire diameter and wire heating on the relationship in (1)

(3) To relate the amount of ozone produced to the magnitude of the corona current

(4) To determine the effect of wire diameter and wire heating on the relationship in (3)

(5) To use these relationships to arrive at the best combination of corona voltage and heating rate to achieve high ion concentrations while complying with the FDA ozone minimization requirement.

II. Literature Review

This research involved the following five major subject areas :

(1) Electrical corona and negative ions

(2) Ozone Chemistry

(3) Research on reduction of ozone formation in coronas

(4) Indoor Air Cleaners

(5) The benefits of negative ions

Each of these areas are reviewed in the following discussion in order to relate each subject area to the overall objectives of the research.

Electrical Corona

Definition and Types

Loeb[6] defined an electrical corona as any of a set of luminous occurrences that appear as a current, in the microampere range, traverses a gap to ground from an electrode of high potential before the final breakdown across the gap occurs. This breakdown or sparking most commonly occurs at a minimum of two times and a maximum of six times the potential of the threshold. The corona threshold potential corresponds to the potential at which the corona current first exists. The current behavior at the threshold consists of intermittent pulses. As the potential increases,

the pulse's frequencies increase which cause a merging of the pulses into a pseudo steady current. Collectively these items make up a phenomena known as the corona onset. Corona current increases linearly with voltage potential at potentials near the starting voltage and parabolically at higher potentials. The word corona comes from the French couronne, meaning crown, a description of one of the forms observed[6].

Negative corona, one type of electrical corona, originates when a high negative potential, placed on an electrode, results in electrons traversing the gap between the electrode and a conductor at ground potential. Electrons flow from high negative to low negative potential or to a positive potential. The electron source, the high negative potential electrode wire, ejects electrons when positive ions formed in the electrical field move toward and bombard the electrode wire surface at high velocities. Further, photo-emission releases electrons by using the photon energy emitted from the ultraviolet light of the corona itself[7,8].

Formation of Negative Ions

The electrons, freed from the electrode, accelerate away from the electrode under the influence of electrical field forces and self field forces (those due to like charge repulsion). The electrons may create negative ions by molecular collisions. The number of negative ions formed depends on the type of gas occupying the space around the

electrode. Gases with high electron affinities, such as, oxygen, chlorine, and sulfur dioxide, readily form negative ions; whereas, nitrogen, hydrogen, and the noble gases - gases with no electron affinity - do not[8].

The negative ion formation may be thought of as electron attachment. As White[8] explains, electron attachment occurs in two ways, each depending upon the gas in the system. In the first way, direct attachment, an electron comes into contact with a gas molecule and adheres to the surface causing the molecule to acquire a higher energy state. This increased energy manifests itself in the form of molecular vibration and/or rotation. The new ion may transfer its energy upon collision with another molecule. After colliding, the gas molecule stabilizes at a lower energy state, since it transferred the energy gained as well as its electron affinity energy. If a newly formed ion does not hit another molecule over a period of time then it may release the electron and become a neutral molecule. This type of electron attachment occurs with oxygen and sulfur dioxide. The indirect method of electron attachment is dissociation. In the first step, an energetic electron splits a molecule apart by colliding with it. Then the electron may attach itself to one of the components of the split molecule. This type of formation occurs with carbon dioxide and water vapor. Carbon dioxide may dissociate when hit by an electron with an energy greater than 5.5 electron volts (eV). If such a

collision takes place, the carbon dioxide splits into an oxygen atom and carbon monoxide and the electron attaches to the oxygen[8]. Oxygen molecules may undergo this same process when struck by an electron with 3.1 to 3.6 eV[6].

Particulate Collection

Upon the formation of negative ions, collection of particulate matter can occur. The particles are collected by charging them which forces them to a grounded surface. The particles can be charged through two mechanisms as discussed by Rose and Wood[7]. The first mechanism, bombardment charging, is similar to the direct form of electron attachment. Particles acquire charge by collision with the negative ions, which are being repelled from the negative electrode by the negative electric field. The amount of charge on the particle depends upon the charging time, its surface area, and the strength of the electric field. The other type of charging, ion diffusion, results from the random motion of the ions causing collisions between the ions and particles. This type of charging depends on the amount of charge transferred which varies as a function of the particle size, gas temperature, gas pressure, gas viscosity, and contact time. When the size of the particles to be collected is less than 0.25 micrometers, ion diffusion becomes an important contributor to particle charging[7].

Benefit of Negative Corona

A negative corona breakdown voltage has been found to

exceed that of a positive corona. In a negative corona, the spark, denoting the breakdown, originates from a region of rather low electric field strength. This region forms because the charge density decreases as a result of charge repulsion from the electrode. Therefore, a high voltage must be applied to bridge the gap. Conversely in a positive corona, the spark originates in a high field region since the negative ions accumulate in the vicinity of the electrode. Therefore, a lower applied voltage will bridge the gap. The differences in the electric field around the electrode causes the breakdown voltage of the negative corona to be up to twice that of the positive corona[8].

Ozone Chemistry

Ozone formation

The amount of ozone produced by the negative corona depends upon the gas phase chemical reaction mechanisms. The ozone molecule consists of three atoms of oxygen in gaseous form. At ambient conditions ozone is unstable and quite reactive. Ozone molecules form naturally in lightning discharges, photochemical reactions, and UV light and artificially in Xerox type copiers, high voltage power lines, faulty wiring, and ozone generators[9].

Theoretically, ozone formation by a corona discharge takes place in two steps. The first step can be initiated by any one of these four reactions[4].

(1) $e^- + O_2 \rightarrow 2O + e^-$ pure dissociation of O_2

(2) $e^- + O_2 \rightarrow O_2^+ + 2e^-$ direct ionization

(3) $e^- + O_2 \rightarrow O^+ + O + 2e^-$ dissociation of O_2 (O^+ formed)

(4) $e^- + O_2 \rightarrow O^- + O$ dissociation of O_2 (O^- formed)

The second step of the process is a reaction involving atomic oxygen, diatomic oxygen, and any other molecule (M) in the gas. The purpose of the third body, M, is to supply or remove kinetic energy[10].

$$O + O_2 + M \rightarrow O_3 + M$$

Unlike reactions in the first step, this reaction has a reaction rate that is dependent upon the gas temperature. Higher gas temperatures lead to lower ozone production rates[4].

Ozone destruction

Temperature is not the only deterrent to ozone production. Atomic oxygen and free electrons react with ozone to produce diatomic oxygen.

$$O + O_3 \rightarrow 2O_2$$

$$e^- + O_3 \rightarrow O_2 + O + e^-$$

These reactions, that convert ozone to diatomic oxygen, become more pronounced at elevated ozone concentrations and

temperatures since ozone becomes more unstable as the temperature increases[9]. Rice and Netzer[9] suggested that ozone decomposition is favored over ozone production above 40 °C. From the work of Amouroux and Goldman[11], as discussed by Viner *et al.*[10], water vapor content of the gas also influences the amount of ozone produced.

$$O + H_2O \rightarrow 2OH^{\bullet}$$

$$OH^{\bullet} + O_3 \rightarrow HO_2 + O_2$$

$$HO_2 + O_3 \rightarrow OH^{\bullet} + 2O_2$$

The water vapor competes for atomic oxygen and the product of this reaction, $OH^{\bullet}$, an intermediate radical that is vibrationally excited, reacts with ozone to form a product that also reacts with ozone to produce diatomic oxygen[10].

Reports on the effect of water vapor on ozone production contrasted. Amouroux and Goldman[11] stated that water vapor decreased ozone production for a positive corona and caused the ozone production by a negative corona to increase slightly. Viner *et al.*[10] found that ozone production by positive corona was enhanced by water vapor and found that an increase in humidity decreased the ozone production by negative corona by as much as 50%.

A number of reaction mechanisms occur that either enhance or hinder ozone production. The sum of all of the reactions that occur under given conditions govern the net

ozone production level. Ozone production depends on the oxygen content of the air, gas temperature, water vapor concentration, and electrical field strength producing the discharge in the gas.

Reduction of ozone formation in corona discharges

Changes in operating procedure

Since positive corona discharges generate less ozone than negative corona discharges, most research investigations with concern for ozone formation use positive corona discharges. Examples of methods for reducing ozone formation in electrostatic precipitators as cited by Castle *et al.*[5] are:

(1) using of the smallest diameter corona electrode wire that will withstand mechanical and thermal stresses without failure.

(2) choosing electrodes that are smooth and round

(3) minimizing the corona current generated while still obtaining the desired collection efficiency

(4) maximizing the flow through the apparatus while still maintaining collection efficiency

(5) eliminating any sharp points or edges and other discontinuities so that uncontrolled discharges do not exist.

Castle *et al.*[5] used a concentric cylindrical geometry and a positive corona in their work. They found a linear relationship between ozone concentration and corona current for a range of air flows and wire diameters. The measured ozone concentrations increased with lower air flows as well as larger wire diameters. Wire sizes ranged from 1.27 to

8.13 mm. Their work showed that the relationships held true for copper, platinum, tungsten, and stainless steel wire electrodes. Wire materials that formed protective oxides performed better over long periods of time. These materials produce a smaller increase in ozone concentrations over time than materials which undergo porous oxidation. The experimentation lead to the formation of a model that accounted for variation in wire diameter, air flow, and current as related to ozone concentrations[5].

Addition of external wire heating

Awad and Castle[3] extended Castle *et al.*'s[5] work by using a wire cylinder configuration and adding external corona wire heating. Since the cylindrical geometry provided a convenient shape to model mathematically, these two men incorporated a temperature rise into the formulation that allowed the prediction that the region around the heated corona wire would experience a voltage drop. The drop in voltage would in turn lead to a reduction in ozone produced per unit corona current. Due to the fact that ozone's instability increases as temperature increases, they realized that ozone would likely be destroyed in the vicinity of a heated wire. The net ozone reduction would depend upon the relative magnitudes of the ozone formation and ozone destruction rates[3].

They experimented with a concentric cylindrical geometry with both positive and negative corona electrode

energization. Several wire materials (stainless steel, bronze, carbon steel, copper, aluminum, Chromel-A, tungsten, and Nichrome) were tested since each material's resistivity would govern the wire heating characteristics. Wire sizes ranged from 0.008 inches (in.) to 0.059 in. The conclusions reached by Awad and Castle[3] were :

(1) Electrode heating power rate increases decreased ozone generation rates

(2) Electrode heating power increases decreased the corona onset voltage

(3) Electrode heating power increased the corona current for a given applied discharge voltage.

(4) With a negative corona the ozone generation rate was 5 to 8 times greater than for positive corona under a fixed set of conditions

(5) Higher resistivity electrode wire material lead to lower ozone production because of the higher heating rates associated with higher resistivity[3].

Ohkubo *et al.*[4] examined the effect of discharge electrode wire heating on ozone formation. A wire-plate type ESP tested with three different electrode wires (0.08 mm stainless steel, 0.3 mm stainless steel , and 0.14 mm Nichrome) was used for the evaluation. These researchers found that the negative corona ozone concentrations were 2 to 2.4 times higher than the concentrations for the positive corona, without wire heating for either type. They reported that the negative corona current was slightly higher than the positive corona current for a fixed voltage. They also found that the maximum ozone concentrations appeared in the region

directly downstream of the corona wire. From a test section traverse, a ozone concentration peak was formed and the base of this peak was narrower for a DC positive corona than an AC corona[4].

For a positive corona, Ohkubo *et al.*[4] found ozone concentration levels decreased as electric heating power increased up to 0.7 W/cm, where the ozone concentration stopped decreasing. Wire heating by the corona discharge current alone did not increase the wire temperature enough to bring about a reduction in ozone level (an increase of up to 5 °C), so reductions required external heating. Using a negative corona, it was shown that a 60% reduction in the steady state ozone concentration level in a room could be achieved if external heating of 0.44 W/cm were applied to the corona wire[4].

Indoor Air Cleaners

Indoor air environment

The importance of the indoor air quality issue in today's society needs no detailed discussion. The widespread use of energy conservation techniques in buildings increases indoor air pollutant concentrations, since ventilation rates are lower[12]. Individuals spend a majority of their time indoors. These factors increase the need to control the quality of indoor air. Interest in clean indoor air also comes from the desire to protect expensive electronic equipment, such as computers[1].

Types of Indoor Air Cleaners

Indoor air cleaners, one method of achieving clean indoor air, remove offending gases and particulate matter. The two main groups of indoor air cleaners are : (1) stationary in-duct cleaners used with forced air HVAC equipment and (2) portable devices that are placed in a room. As of 1982, the production of the portable type had lead to a market of $150 million per year[12].

Godish[1] described the major types of indoor air cleaners on the market today. There are three basic forms of electronic air cleaners. The largest subgroup is the "ionizing plate type." This type of air cleaner uses a two-stage approach, one step for charging and the other for collection. The air is ionized by flowing past high potential positive wire electrodes. The ionized air charges particles by colliding with them. The ionized particles are then collected on negatively charged plates. The second type called the "charged media non-ionizing type" combines both electronic air cleaning and filters. This class consists of a filter media supported by a metal frame that has members of alternating charge. This type of cleaner combines the charging and collection processes. The filter forms an electrostatic field which polarizes the particulate matter so that the charged particles are drawn to the filter. The third type known as the "charged media ionizing type" ionizes the air flow when it passes through a corona discharge. The

charged particles are then collected by a filter of opposite charge[1].

Fan-filter types

Many small indoor air cleaners use fans and filters. Godish[1] explained that these consist of a high-velocity fan and a dry fiber filter that may be treated with a scented medium to mask odors. Also, electrostatic charges may be employed to aid particulate capture. The most effective type of the fan-filter combination uses the HEPA (high efficiency particulate arrester) system. A HEPA filter is a high-density filter made up of fine diameter fibers. Since the HEPA filter can easily be fouled by large particles, a prefilter, a lower density filter, is usually located upstream of the HEPA[1].

Negative ion generators

The other popular small indoor air cleaner uses the concept of negative ion generation. Negative ion generators expel a constant stream of negative ions which charge the particles in the air upon collision. The like charges placed on the particles cause them to repel each other until they hit walls and/or other surfaces where they are collected. Of course, this soils the walls and furniture of the room. Because of this problem, some negative ion generators produce ions in pulses. When ions are not being ejected from the filter the negative charged particles are drawn back to the positive charged outer covering of the generator[1].

Effect of negative ions on the human body

Before negative ion generators were used as air cleaners they were marketed in the 1950's and early 1960's as a type of health machine. This came about by theories that negative ions produce positive feelings in humans. These machines were forced off the market by the Food and Drug Administration because the claims could not be verified[1].

Jokl[13] described the reaction of the human body to negative ion concentrations. These reactions include a shift of the pH of the blood to the alkaline range, a decrease in blood pressure, a decrease in oxygen consumption, decomposition of serotonin by 5-hydroxyindolacetic acid, and an increase in the ciliary motion in the throat and mucous membrane activity. Jokl[13] cited work performed in 1976 which concluded that negative ions decreased serotonin (5-hydroxytryptamine) levels in the midbrain. These lower serotonin levels are believed to be responsible for the tranquil feelings that result when one is exposed to negative ions. Also, high negative ion concentrations increase the virus resistance of the body because the ions destroy bacteria and fungus and lower liquid aerosol concentrations[13]. Jokl[13] further explained that serotonin levels affect sleep patterns and a person's mood due to their role in nervous impulse transmission. High serotonin levels intensify secretions in the blood, metabolism, and interactions between the nervous and circulatory system. High

concentrations of this substance exist in the poisons of wasps and scorpions. Therefore, lowering the serotonin levels produce a calming affect on the body. Negative ions were used to evaluate sleep at Stanford University and psychoneurosis and anxiety problems at Buenos Aires University. In both studies beneficial effects were found, most likely due to the lower serotonin level facilitated by the anions[13].

Effect of ion concentration on air perception

The concentration of positive or negative ions in the air can cause a sensation that the air is stale or fresh. As discussed by Osborn[14], high levels of positive ions can cause feelings of uneasiness and tiredness. These levels exist in crowded areas with poor ventilation as well as at the onset of a thunderstorm. High levels of negative ions exist in mountainous areas, near the ocean and waterfalls, and in country areas. They reportedly produce pleasant feelings. Negative ions neutralize positive ions, but must be generated by a portable system that can be placed in the area where the high positive concentration is located because the negative ions react with ductwork in an in-duct system[14].

III. Methods and Materials

The experimental setup, a descriptive overview of the research, and the methodology used to compile the data, are discussed in this chapter.

The test section consisted of Plexiglas and was assembled using methylene chloride to melt the sections together. However, the top section was hinged with duct tape so it could be opened to change wire size or to repair broken wires. Plexiglas was used because it allowed for easy viewing of the contents and provided a nonreactive wall material. The test section dimensions were 10 centimeters (cm) wide, 11 cm high, and 63 cm long.

An Archer® Cooling Fan (model 273-241C) made by Tandy Corp. (Fort Worth, TX) was bolted to the inlet of the test section. The fan pulled the air into the test section. A sharp edge orifice manufactured by General Metal Works (Village of Cleves, OH), placed upstream of the fan, provided flow rate data. The pressure drop across the orifice was measured with a Dwyer® manometer (Dwyer Instruments Inc., Michigan City, IN). The pressure drop range of 0 - 0.25 inches of water across the orifice corresponded to a volumetric flow rate, obtained by calibrating the orifice (see Appendix B for calibration data and curve). The orfice

was calibrated with a linear flow meter.

The negative corona discharge electrodes (high voltage wires) and a grounded screen were positioned inside the test section as illustrated in Figure 2. The discharge wires were made of Nichrome, a 60/40 nickel chromium alloy. Two wire gage sizes (32,38) having diameters of 0.2 and 0.1 millimeters (mm), respectively, were purchased from Pelican Wire Co. (Naples, FL). The remaining Nichrome wire size of 0.32 mm (28 gage) was made by Consolidated Wire (Chicago, IL) and its metal composition was not known. All of these wires were supported by a plexiglass frame which had glass tubing glued to it through the use of epoxy. The grounded screen consisted of 18 gage copper wire which was soldered together in a grid pattern, as illustrated in Figure 1, with the bars being approximately 2.5 cm apart. Inside the test section was also a fine wire mesh ion collection screen supported by a 1 inch wire mesh with a plexiglass base. This was used to measure the amount of negative ions that passed the ground screen.

The high voltage to the discharge wire came from a custom made transformer (Transformer/Electric Company, Roanoke, VA) with an input voltage of 110 Volts (V) and an output potential of 20 kV. The sinusoidal voltage wave was half rectified with a diode and the voltage peaks were lowered using two capacitors (8100 picofarads (pF), 8350 pF) in parallel as seen in Figure 3. These devices were then

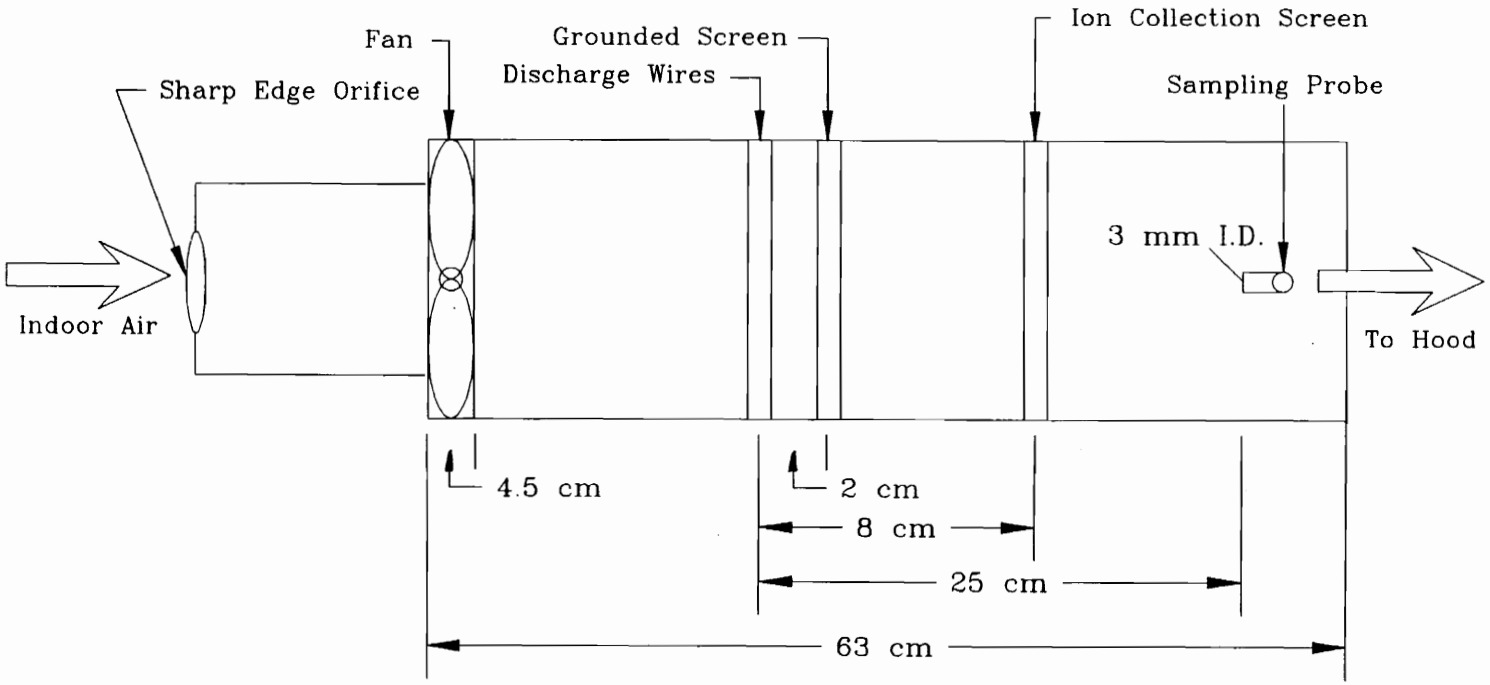

Figure 2. Experimental Test Section

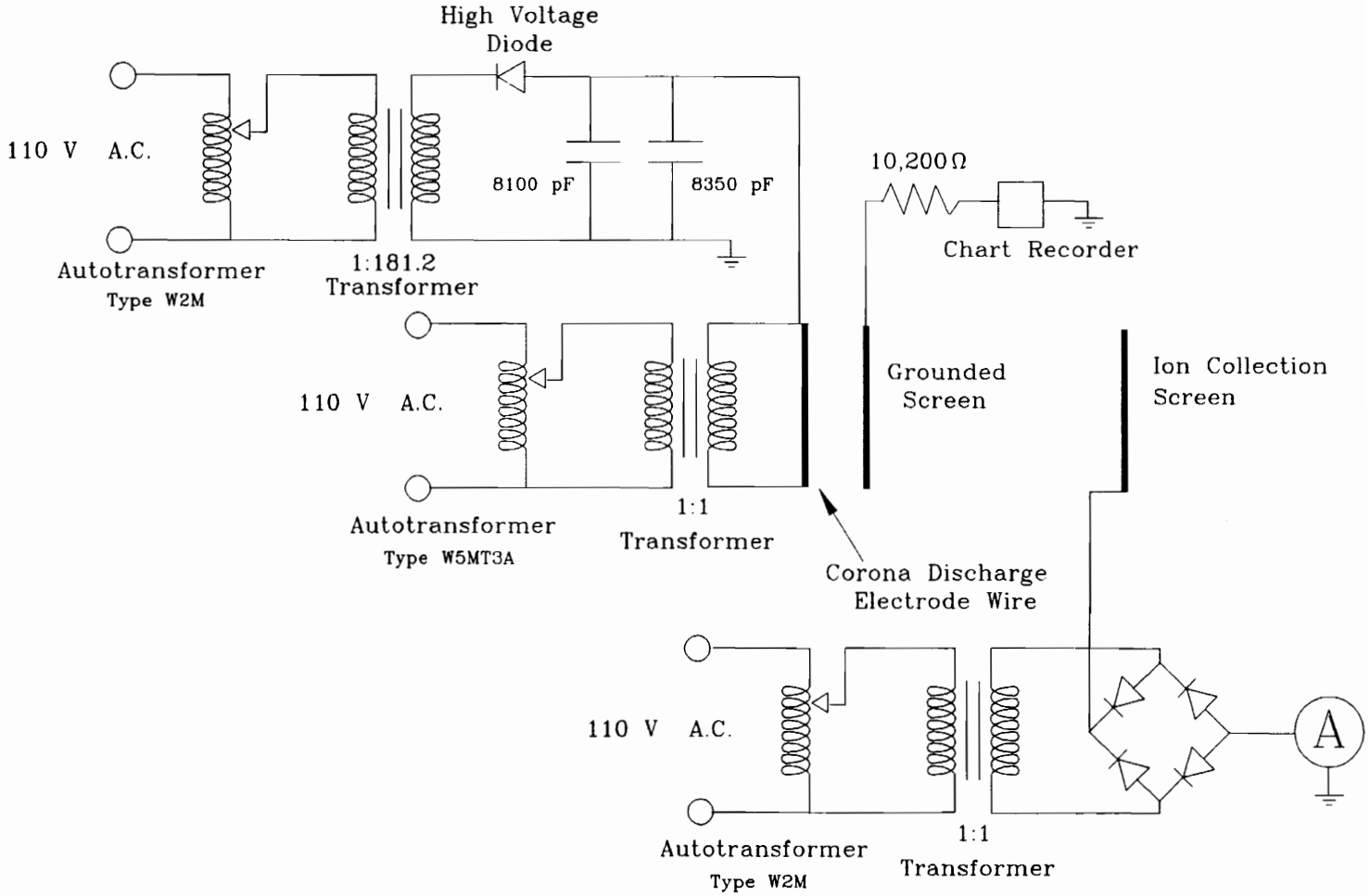

Figure 3. Electrical Schematic for Wire Screen Experimental Apparatus

connected to one side of the electrode discharge wire. The input voltage supplied to the transformer was varied using a VARIAC® autotransformer type W2M (General Radio Company, Cambridge, MA). As discussed by Ohkubo *et al.*[4], heating of the electrode wire by the corona itself only increased the temperature by a few degrees Centigrade. Therefore, external wire heating would be necessary to raise the wire surface temperature further. External heating power for the corona wire was supplied by a 1:1 transformer with 20 kV isolation made by Transformer/Electric Co. The transformer was connected to both sides of the electrode making a closed circuit. The resistance of the Nichrome wire transformed the electrical power into thermal energy which heated the wire. The input voltage to this transformer was controlled by a METERED VARIAC® autotransformer type W5MT3A made by the General Radio Company. A potential of +100 V was placed on the ion screen using another VARIAC® autotransformer type W2M, a Ultra-Isolator model 11T255R made by Topaz Electronics (San Diego, CA), and a full wave rectifier.

Ozone concentrations were detected by UV light absorption with a Dasibi 1003-RS ozone monitor (Dasibi Environmental Corp., Glendale, CA). The monitor was calibrated with an EPA approved ozone generator (see Appendix B for a description of the calibration procedure, calibration data and the calibration curve). An L-shaped glass sampling probe (I.D. of 3 mm) was placed in the test section (see

Figure 2) and was connected to the monitor using Teflon tubing.

Fluctuations in the corona current were measured by a Single Channel Recorder BD8 made by Kipp & Zonen (Delft, Holland) in series with a 10,200 ohm resistor. The current passing through the ion screen was measured using a Micronta® 25 range multitester (273-241C) made by Tandy Corp. The temperature in the lab and the humidity level were measured using a sling psychrometer made by Bacharach Instruments (Pittsburgh, PA).

The following discussion describes a typical sample run. First, the wire size to be analyzed was placed in the framing device. The ends of the wire were connected to two bolts that went through the test section and were connected to both the high voltage and external heating apparatus. The grounded screen (see Figure 2) was then placed 2 cm away from the discharge wire and the ion screen 8 cm away. The distance from the discharge wire to the sampling probe was 25 cm. The temperature, humidity, and barometric pressure in the room were measured. All electric apparatus was connected to the laboratory power supply. The ozone monitor ran continuously to assure that the monitor was thermally stable and maintained at the calibrated operating conditions.

The fan was started and allowed to run for 5 minutes, so that a constant flow was developed through the test section. The chart recorder was turned on, zeroed, and placed on

standby. A potential of +100 V was placed on the ion screen. After the five minutes, 10 ozone concentrations were read from the ozone monitor, each measurement separated by the sampling time of the monitor, approximately 25 seconds. These measurements were taken for the background ozone concentration. If the sampling run called for wire heating then the desired heating power level was placed on the wire before the background measurements were taken. The chart recorder was then taken off standby (chart paper was allowed to move). Then a voltage was applied to the corona wire that gave a constant response on the chart recorder. The voltage applied and the chart recorders sensitivity range were noted on the chart paper. The corona was allowed 5 minutes to stabilize, the chart paper was marked for the starting point, and then 10 readings were again taken from the ozone monitor. After the ten readings, the end of the run was marked on the chart paper and the discharge voltage stopped being applied. The chart recorder would then be rezeroed and placed on standby. Then the next voltage level would be applied, usually 1000 V greater than the previous reading, and the 10 readings would be taken after the five minute waiting period. These iterations continued until the corona arced or the ozone levels were seen as extremely high (measured ozone concentration - background ozone level > 50 ppb). All data collected from a run was tabulated as shown in Table 1. The data tables for subsequent runs are presented in Appendix A.

Table 1. Data Collection Performed on 9/24/92 RUN #1

Flow	Voltage Potential	Corona Current	Heating Power	Ozone Production (ppb)												Ion Current
cfm	kV	μA	W	1	2	3	4	5	6	7	8	9	10	AVG	std dev	μA
7.0	---	---	---	19	21	15	25	17	24	24	24	22	18	20.9	3.30	---
7.0	9.5	0.74	---	25	22	16	26	24	20	21	21	20	20	21.5	2.77	---
7.0	10	2.0	---	32	24	32	28	27	24	24	28	20	23	26.2	3.71	0.3
7.0	11	8.6	---	44	49	44	44	45	39	48	50	43	45	45.1	3.05	0.3
7.0	12	20	---	86	84	87	88	77	86	89	88	82	85	85.2	3.37	1.0
7.0	13	60.7	---	199	198	189	223	216	189	203	216	178	226	204	15.2	2.0

Wire Diameter = 0.1 mm Sampling Flow Rate = 2 LPM
Screen Spacing = 8 cm Ground Spacing = 2 cm Sampling Spacing = 25 cm
NOTE : All spacing distances in reference to corona wire

Ion Screen Potential = 100 V
Temperature = 19.4 °C Bar. Pressure = 718 mm Hg Humidity = 52.5% R.H.

In order to graphically display the data, the ozone readings and corona current were averaged. The ten ozone concentrations were averaged and the standard deviation was calculated. For the corona current, the strip chart section to be averaged was measured with a ruler from the starting mark to the ending mark on the chart paper. Then over this region an average line was drawn for each unique subsection found. Each of the subsections were measured and their value was weighted using the subsection length. All subsection values were then added together and divided by the total section length. This method was basically a graphical integration procedure.

The external heating of the corona wire began at a wire temperature of 40 °C and ended at 100°C with 20° increments. Once external heating was added to the wire, the wire was allowed to stabilize for five minutes. The external heating would be maintained throughout the entire experiment. All runs performed on a wire size were done in one day (i.e. room temperature, 40 °C, 60 °C, 80 °C, and 100 °C). In order to calculate the amount of power needed for a particular temperature to be reached, a FORTRAN program was written. Appendix C contains the program statement listing. The program was based on the equations describing natural (free) and forced convection over a circular wire. These equations were adapted from an Appendix presented by Ohkubo *et al.*[4]. The equations were developed by Morgan[15] and Chang and

Laframboise[16]. Through the use of this program, target input power levels were obtained using representative values for room temperature and wire length as listed in Table 2. After the experiment was completed, the program was again applied using the actual conditions as input in order to estimate the actual wire surface temperature.

Table 2. Target Input Power Levels and Corresponding Wire Surface Temperatures

Wire Diameter (mm)	Wire Length (m)	Wire Surface Temperature (°C)	Power Input (W)
0.1	0.7	40	4.8
		60	13.6
		80	25.0
		100	39.2
0.2	0.7	40	5.1
		60	14.2
		80	26.1
		100	40.6
0.32	0.7	40	5.3
		60	14.8
		80	27.0
		100	41.9

IV. Results

This chapter presents the data collected in the three experiments, which each had five separate parts. Appendix A presents the raw data for all the trials in a tabular form. Appendix A also contains tables to illustrate the manipulation of the data into the form presented graphically in this section.

The Corona Current and Voltage Relationship

The nonlinear relationship between the corona current and applied voltage can be seen in Figures 4-6. In these figures, the presence of the onset voltage begins with the parabolic lines at some point above 6 kilovolts (kV). Note that the curve shifted to the left as the wire surface temperature increased, which indicated that the onset voltage was reduced. This behavior was consistent for all wire sizes evaluated as indicated by the curves.

Reduced onset voltage accompanied a reduction in wire size. For all of the wire surface temperatures used, the line traced by the current/voltage relationship was shifted to the left as the wire size was reduced as seen in Figures 7-11. These figures also indicated that higher currents are generally achieved with a smaller diameter wire.

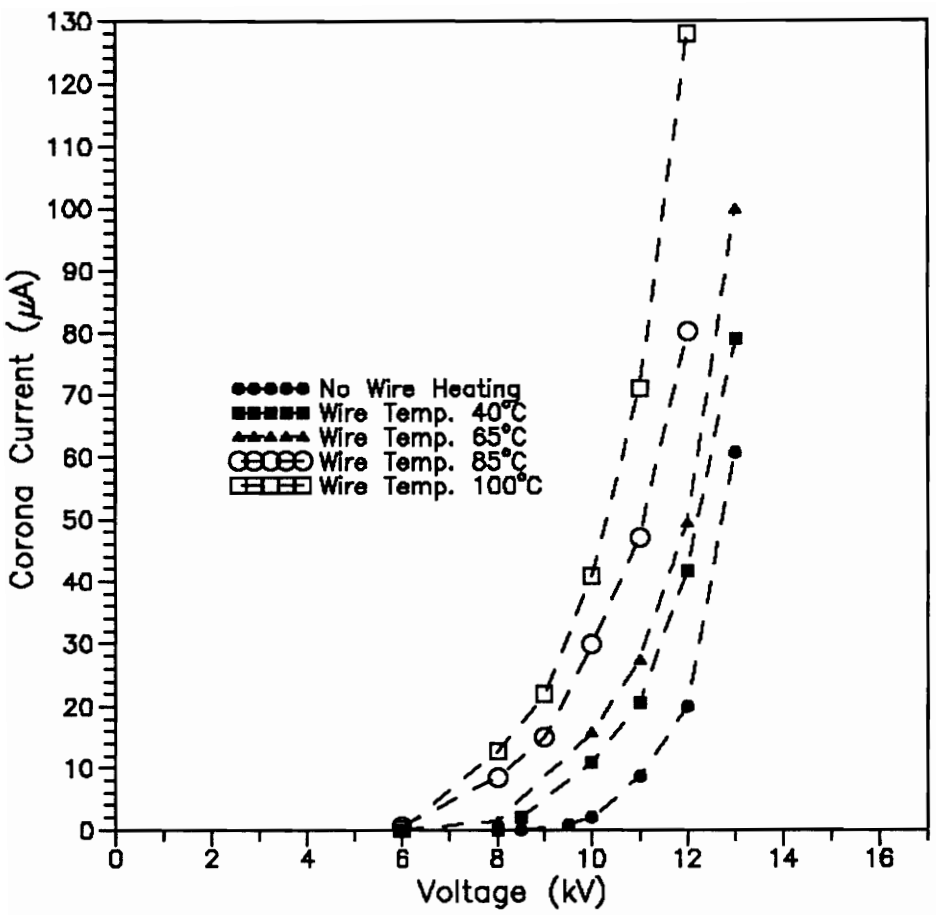

Figure 4. Corona Current vs. Voltage for 0.1 mm wire (2 cm gap, 52 - 69% R.H.)

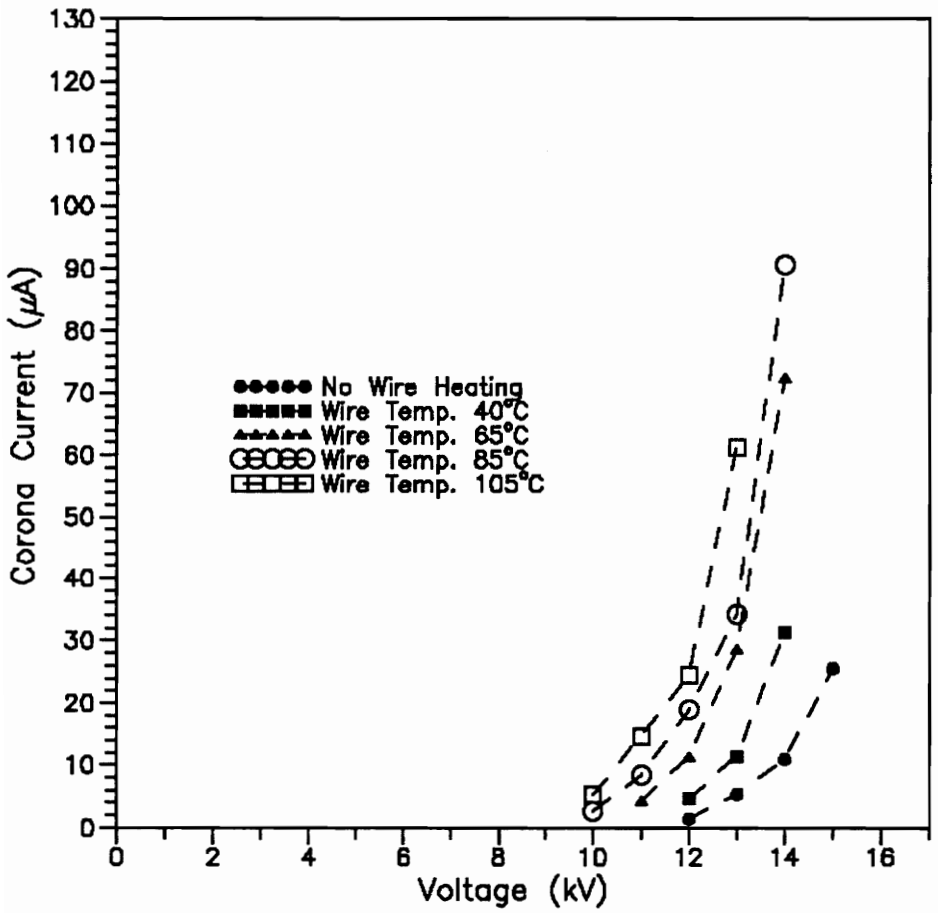

Figure 5. Corona Current vs. Voltage for 0.2 mm wire (2 cm gap, 60 - 68% R.H.)

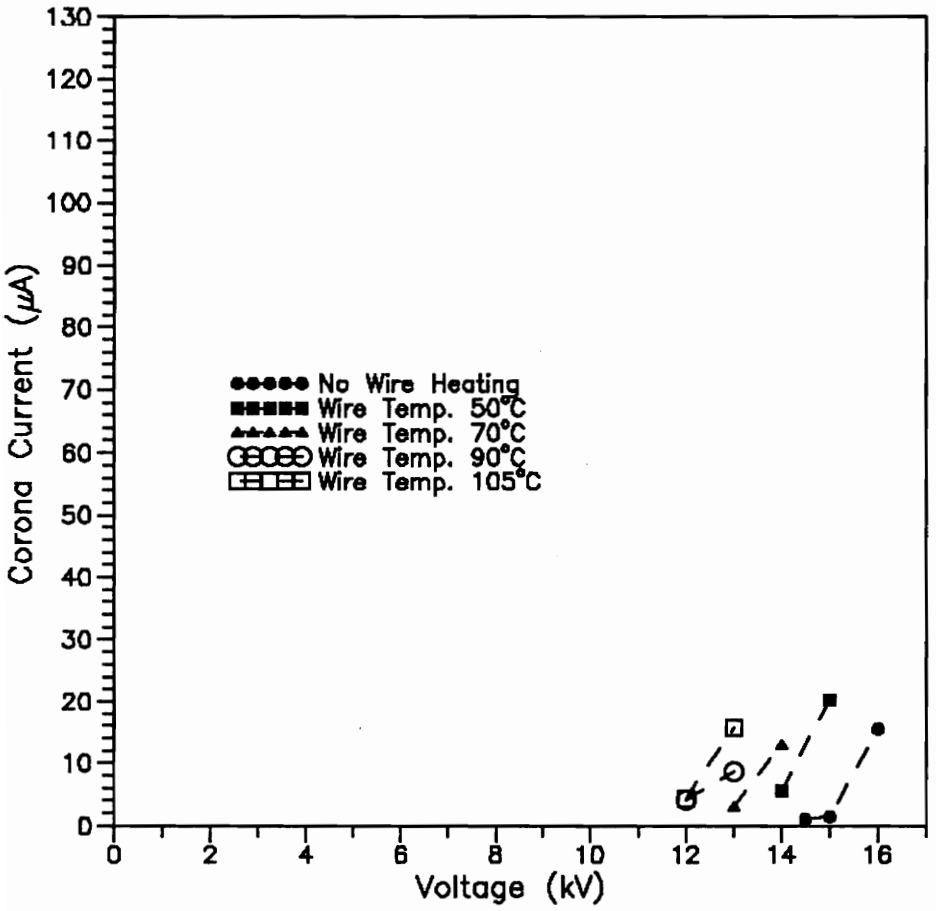

Figure 6. Corona Current vs. Voltage for 0.3 mm wire (2 cm gap, 41 - 47% R.H.)

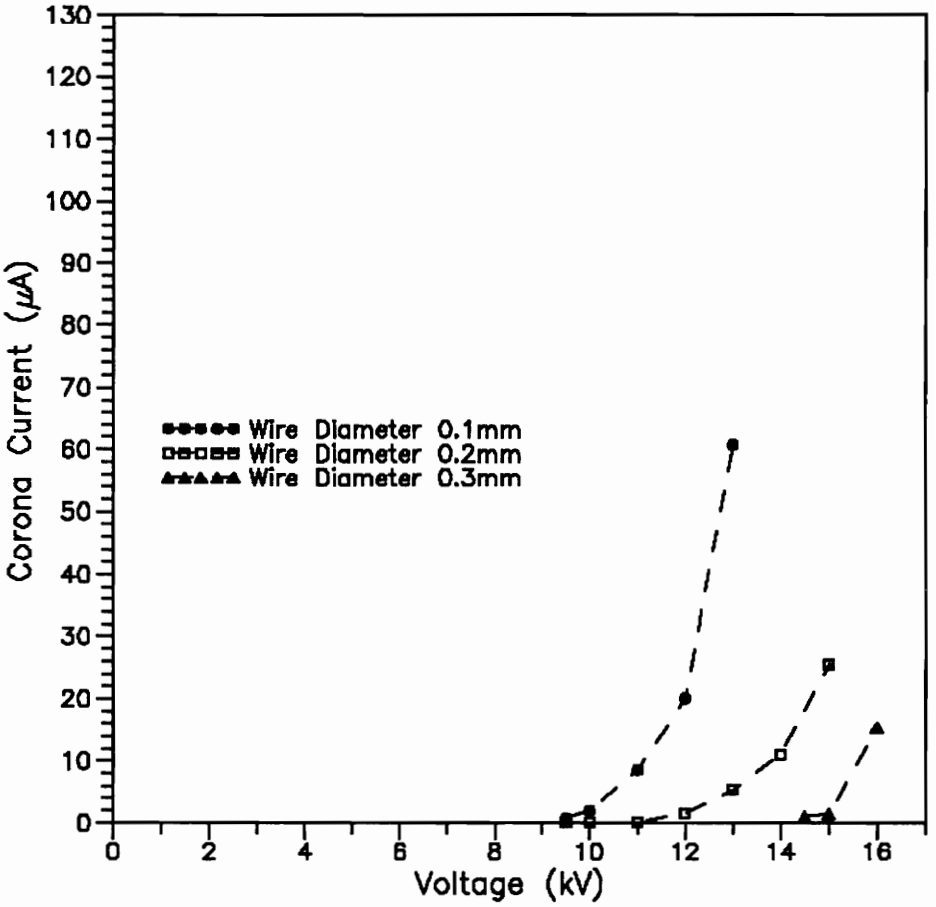

Figure 7. Corona Current vs. Voltage
No external wire heating

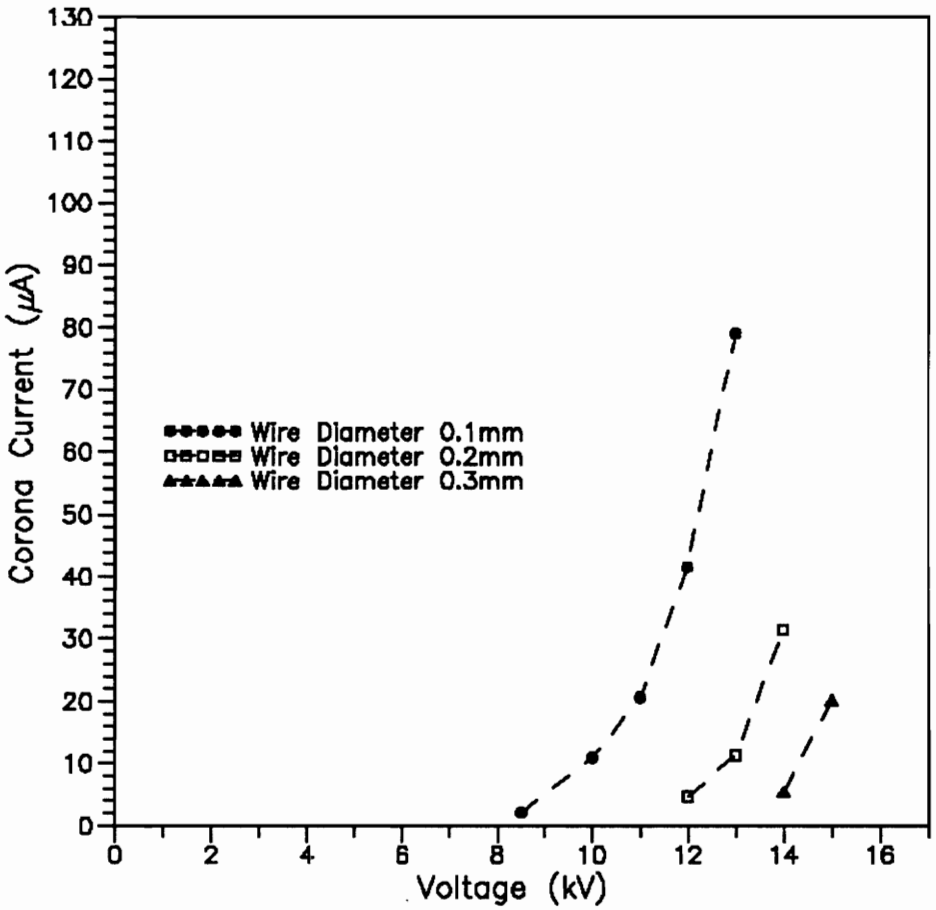

Figure 8. Corona Current vs. Voltage
Wire Temperature 45 °C

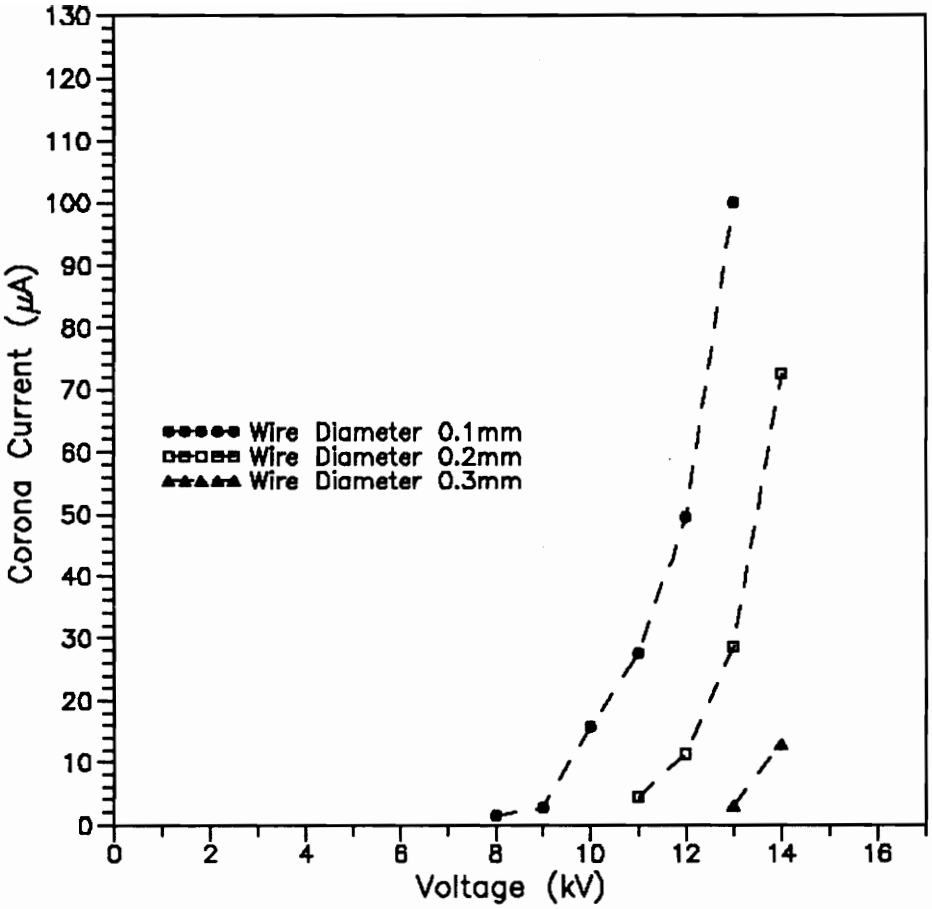

Figure 9. Corona Current vs. Voltage
Wire Temperature 70 °C

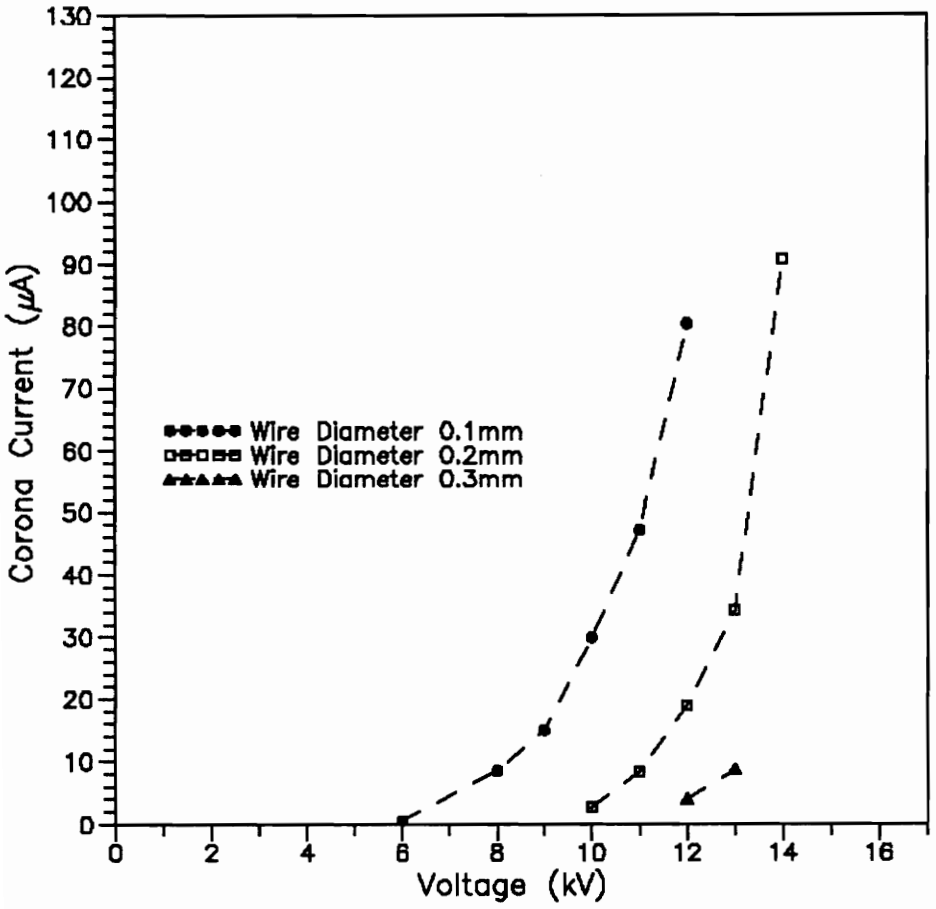

Figure 10. Corona Current vs. Voltage
Wire Temperature 85 °C

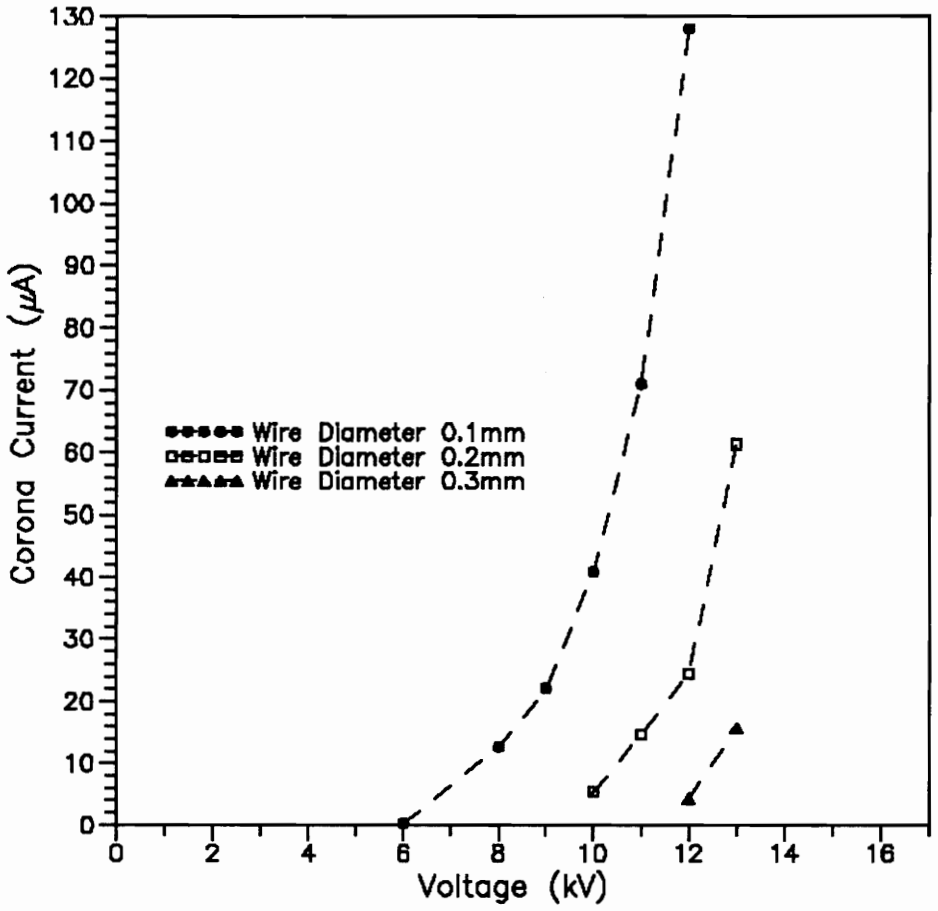

Figure 11. Corona Current vs. Voltage
Wire Temperature 105 °C

The Ozone Concentration and Corona Current Relationship

The relationship between the ozone concentration and the corona current over the range examined was found to be linear. For a given temperature, the ozone concentration increased with the corona current. For a given wire size, the slope of the line produced by interrelating the ozone concentration and current decreased as the temperature increased up to a limiting value. This phenomena can be seen for all wire sizes used in Figures 12-14. Note that the ozone concentration dropped as the wire surface temperature increased.

A reduction in ozone concentration occurred as wire size decreased. For all wire surface temperatures tested, the slope of the line traced by the ozone/current relationship was lower for a wire of smaller diameter (see Figures 15-19). The slopes of these lines are compared in Table 3.

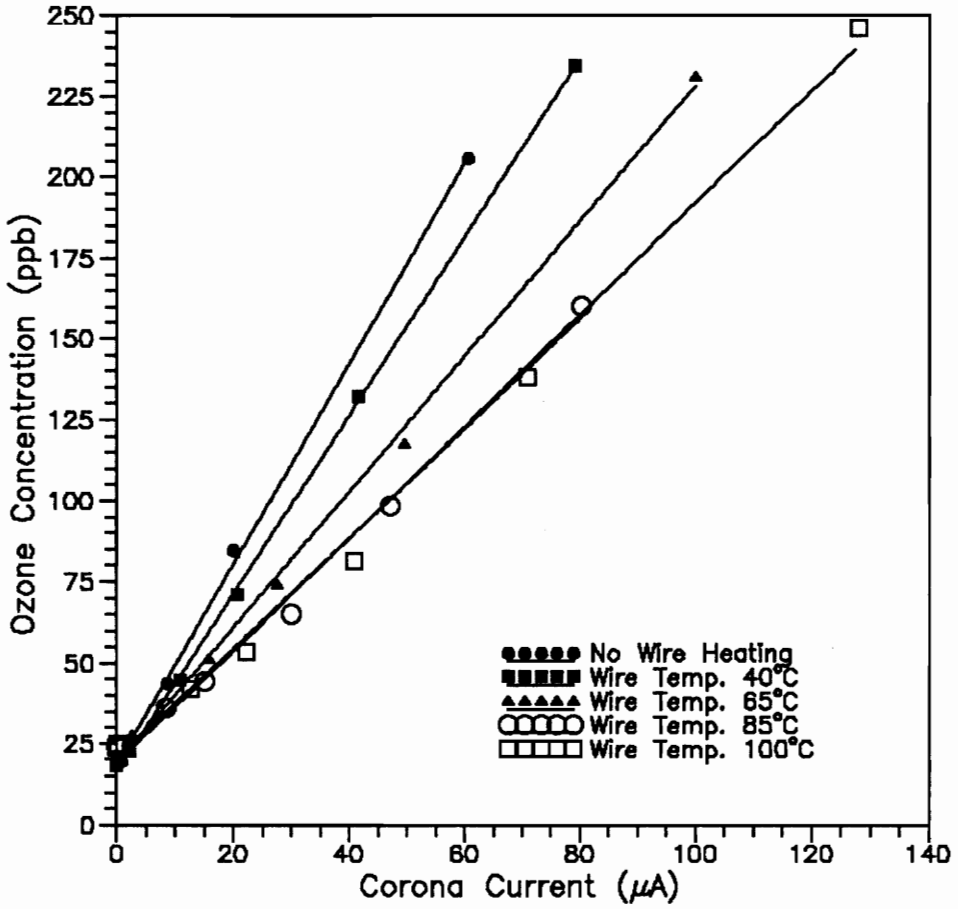

Figure 12. Ozone Concentration vs. Corona Current for 0.1 mm wire (2 cm gap, 52 - 69% R.H.)

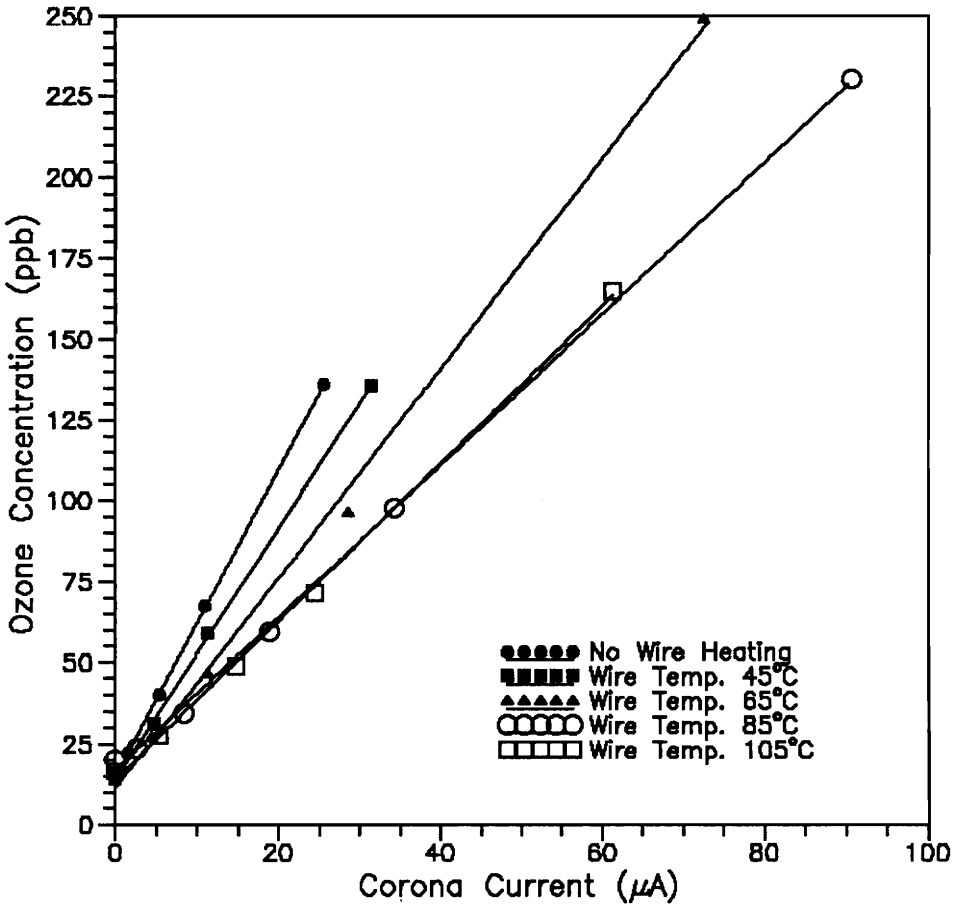

Figure 13. Ozone Concentration vs. Corona Current for 0.2 mm wire (2 cm gap, 60 - 68% R.H.)

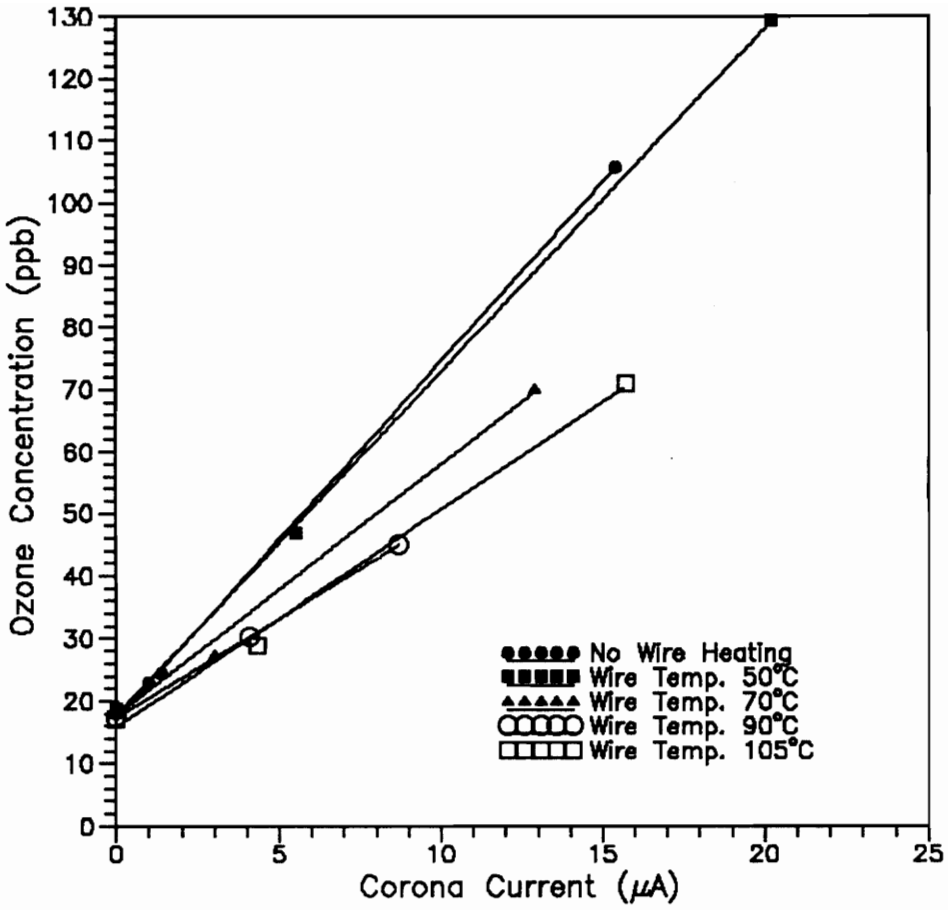

Figure 14. Ozone Concentration vs. Corona Current for 0.3 mm wire (2 cm gap, 41 - 47% R.H.)

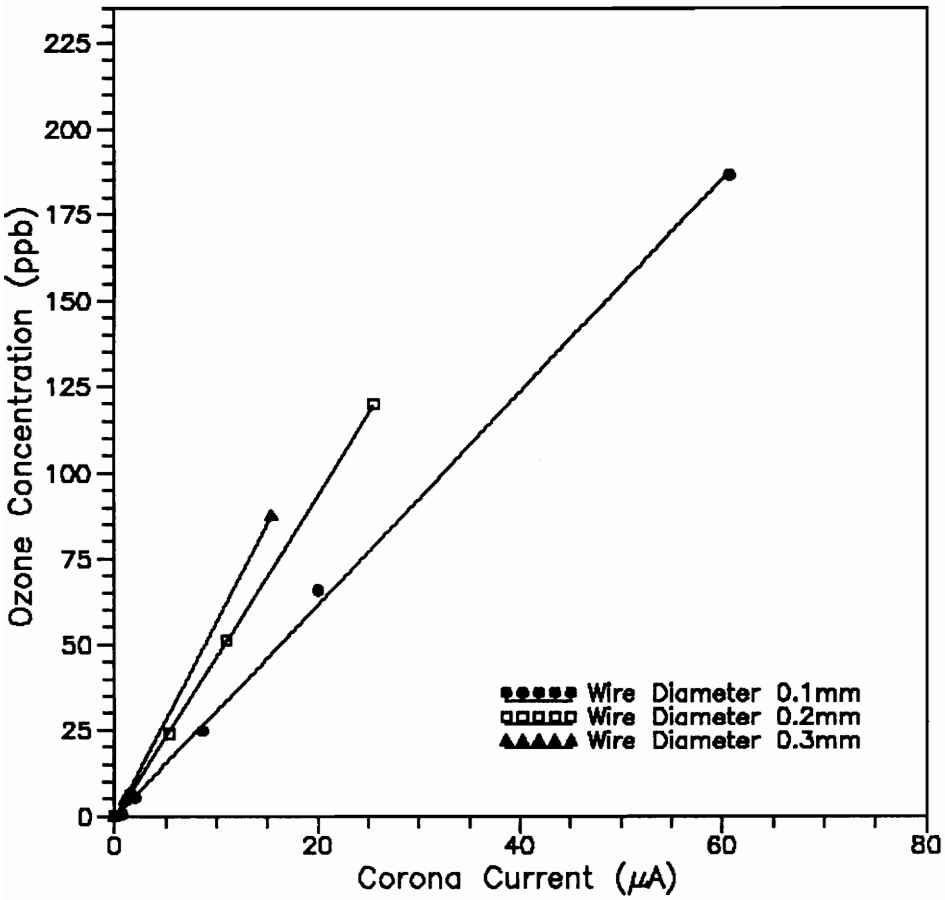

Figure 15. Ozone Concentration vs. Corona Current
No external wire heating

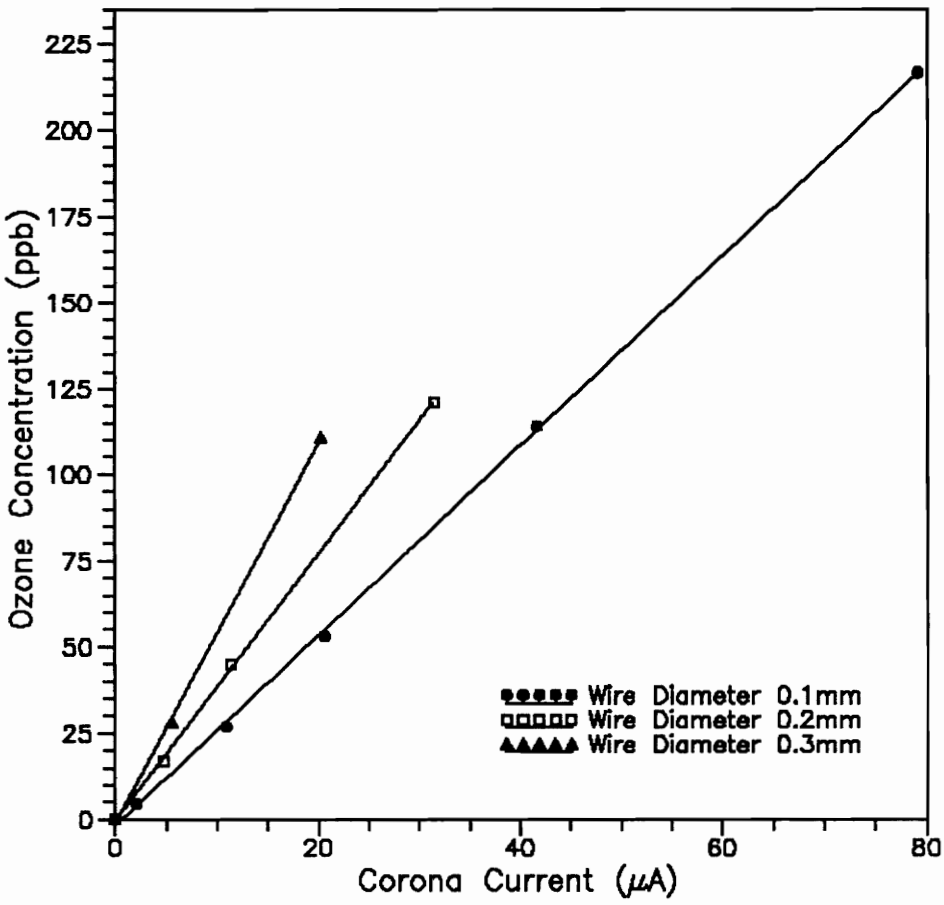

Figure 16. Ozone Concentration vs. Corona Current
Wire Temperature 45°C

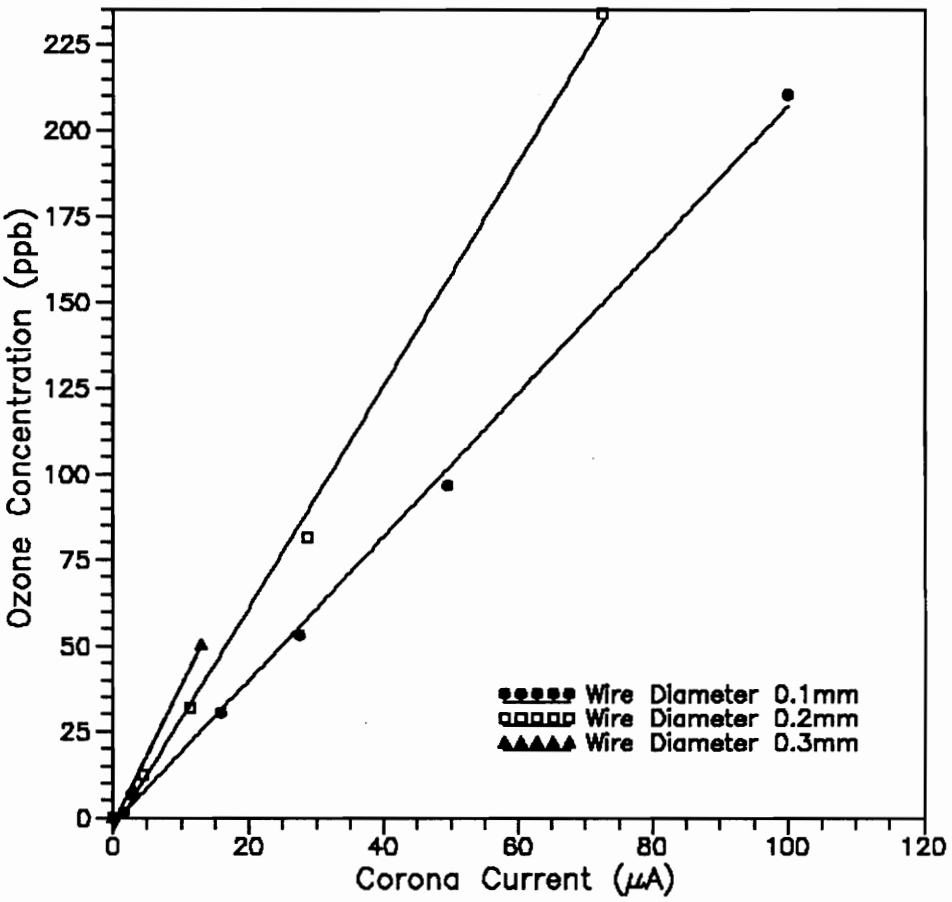

Figure 17. Ozone Concentration vs. Corona Current
Wire Temperature 70°C

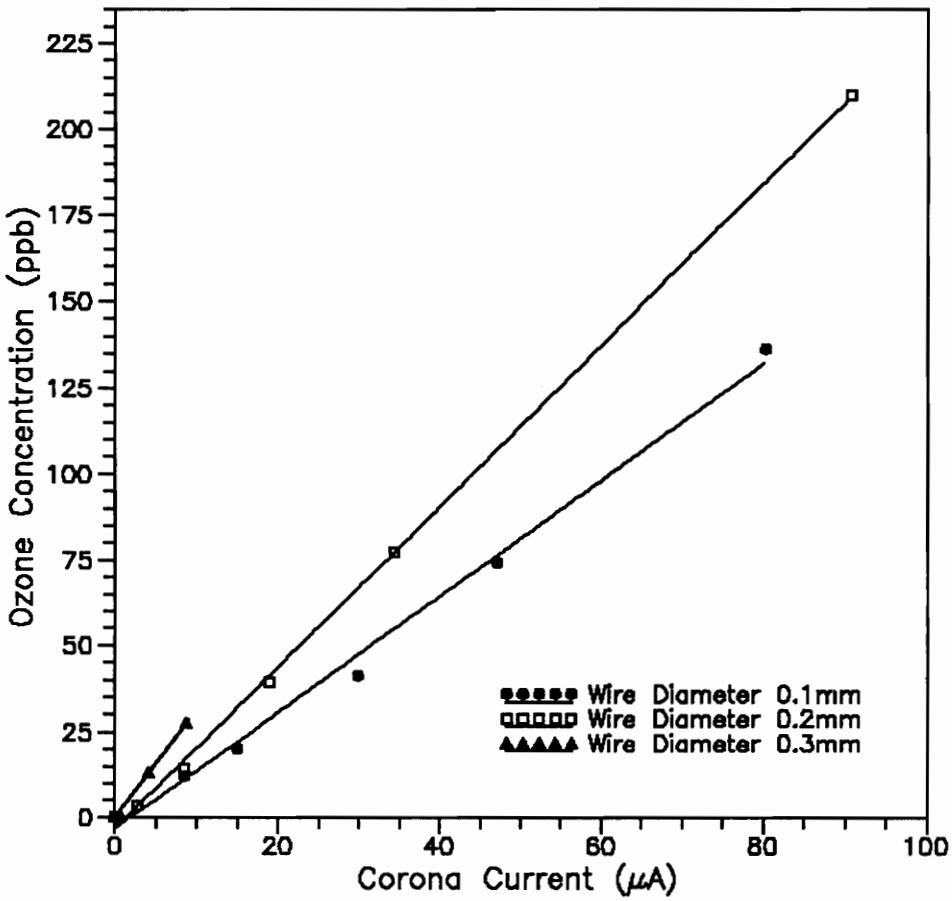

Figure 18. Ozone Concentration vs. Corona Current
Wire Temperature 85°C

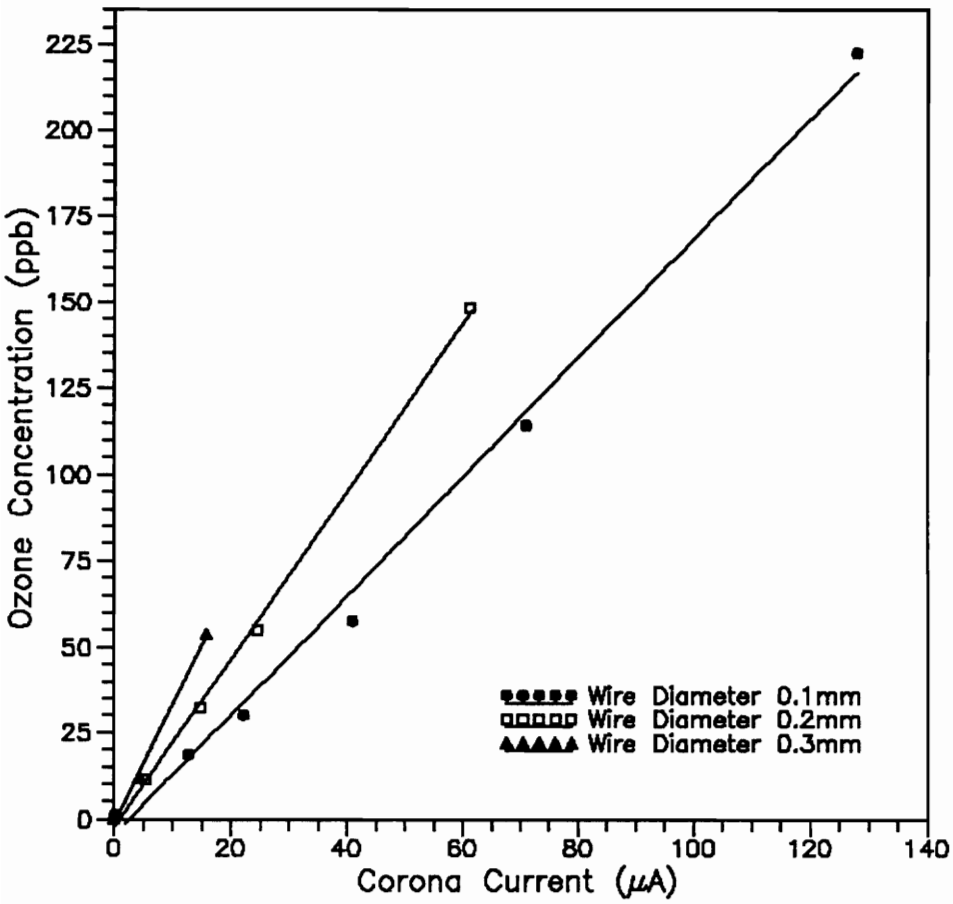

Figure 19. Ozone Concentration vs. Corona Current
Wire Temperature 105°C

Table 3. Equations of lines on Figures 15 - 19

Wire Size (m)	Temperature (°C)	Equation
0.0001	*	Y = 3.09*X - 0.35
	45	Y = 2.76*X - 1.73
	70	Y = 2.09*X - 1.84
	85	Y = 1.69*X - 3.2
	105	Y = 1.73*X - 4.48
0.0002	*	Y = 4.73*X - 0.85
	45	Y = 3.87*X - 0.18
	70	Y = 3.24*X - 3.66
	85	Y = 2.34*X - 3.07
	105	Y = 2.43*X - 2.16
0.00032	*	Y = 5.74*X - 0.8
	45	Y = 5.51*X - 0.94
	70	Y = 4.02*X - 1.85
	85	Y = 3.17*X + 0.03
	105	Y = 3.48*X - 1.42

* - Room Temperature (No Wire Heating)
Y - Ozone Concentration (ppb)
X - Corona Current (μA)
Slope - ppb/μA

V. Discussion

This chapter discusses the results presented in Chapter IV. Information reported in this section consists of both information obtained from this research and information reported in past research publications.

The Corona Current and Voltage Relationship

The nonlinear relationship that resulted from the experiments performed in this research was typical of the results found by other investigators. The relationship was described by H.J. White[8] for a concentric wire and cylinder design. It was important to discover that the current/voltage relationship for the wire to plane screen geometry, used in this research, followed that of an ESP.

This research also showed that even though the geometry was different, the same phenomena occurred when the wire size was reduced and the wire surface temperature increased. Results obtained in this research agreed with those observed by Awad and Castle[3] in their concentric electrostatic precipitator experiments.

Effect of external wire heating and wire diameter on corona current

Using the equations found in the results section (Table 3) with the ozone concentration (Y) equal to 50 ppb, the increase in the corona current due to external heating and

varying wire size were found. A 79% increase in the corona current was achieved for a 0.32 mm Nichrome wire at 89°C compared to the same wire at room temperature. For a 0.2 mm Nichrome wire at 84°C, a 110% increase resulted. The 0.1 mm Nichrome wire at 84°C gave an increase of 93% (see Table 4 for more detail). When each discharge wire was compared to the others without external wire heating, changing from a 0.32 mm wire to a 0.2 mm wire resulted in a corona current increase of 22%. When the wire was reduced further from 0.2 mm to 0.1 mm, an increase of 51% resulted. If the smallest and largest wires are compared, a 84% increase in corona current resulted (see Table 5).

Table 4. Current Increase due to External Heating

Wire Size (mm)	Temperature (°C)	Corona Current (μA)	% Increase
0.3	*	8.85	0
	49	9.25	5
	73	12.9	46
	89	15.8	79
	103	14.8	67
0.2	*	10.8	0
	43	13.0	20
	66	16.6	54
	84	22.7	110
	106	21.5	99
0.1	*	16.3	0
	38	18.7	15
	65	24.8	52
	84	31.5	93
	99	31.5	93

* - Room Temperature (No Wire Heating)

Table 5. Current Increase due to Wire Diameter

Wire Size (mm)	Corona Current (μA)	% Increase wrt 0.3	% Increase wrt 0.2
0.3	8.85	0	*
0.2	10.8	22	0
0.1	16.3	84	51

* - 22% decrease

The Ozone Concentration and Corona Current Relationship

The relationship between the ozone concentration produced and the corona current flow was a critical result obtained from this research. This was because one objective of this research was to find the optimum operating conditions of a negative corona design that would meet the FDA requirement that no more than 50 ppb ozone be emitted from such a device.

Effect of wire diameter on ozone concentration

General trends in the Ozone/Current relationship found in this study agreed with those observed by Castle *et al.*[5]. In this new set of experiments, lower ozone concentration levels were produced as the wire size was decreased; even though, the geometry tested was radically different from earlier studies. For this research, a 18% ozone reduction resulted from using a 0.2 mm wire instead of a 0.32 mm wire and a further decrease in the wire size to 0.1 mm resulted in a 34% reduction (see Table 6). These percentages were found using the slopes of the lines of Figure 15 (no external wire heating), that appeared in the results section, and using the

Table 6. Ozone Reduction due to Wire Diameter

Wire Size (mm)	Current (μA)	Ozone (ppb)	% Reduction wrt 0.3	% Reduction wrt 0.2
0.3	16.3	92.8	0	*
0.2	16.3	76.2	18	0
0.1	16.3	50	46	34

* - 18% increase

highest corona current, of all wire sizes, that resulted in an ozone concentration of 50 ppb. These lines were chosen because the conditions with no wire heating were the most reproducible and 50 ppb was chosen because this was the FDA limit. If the smallest and largest wire sizes are compared, a 46% decrease in the ozone production was observed.

Castle *et al.*[5] presented graphs of ozone concentration versus corona current as a function of wire diameter for a concentric cylinder type wire precipitator. The electrode wire material was copper and the experimental flow rate was 2.36 liters/second (l/s). The slopes of the lines obtained by these researchers that were close to wire sizes tested in this research were 0.62 parts per billion/microampere (ppb/μA) for a 0.09 mm wire and 1.42 ppb/μA for a 0.25 mm wire. As seen in Table 3 of the results section, this study, which used the wire to plane screen geometry and a 3.3 l/s flow rate, found a slope of 3.09 ppb/μA for a 0.1 mm Nichrome wire and 4.73 ppb/μA for a 0.2 mm Nichrome wire. Therefore, a higher ozone generation rate per μA was found in this

study.

This higher ozone production rate was evidently caused by the differences in geometry. As discussed by Viner *et al.*[10], in a concentric type of wire duct precipitator a boundary layer is formed along the length of the electrode because the electrode is parallel to the air flow. In this low turbulence region, the newly formed ozone can react with other ozone molecules created further downstream and cause the reformation of oxygen molecules. In a geometry where the electrode was normal to the air flow, such as the one studied in this research, the ozone molecules are swept away from the electrode and are diluted in the surrounding air. Therefore, the probability of collision with other ozone molecules was lowered and a higher ozone production rate per μA resulted.

Effect of external wire heating on ozone concentration

The results from external wire heating found in this research also agree with the general trends found by Awad and Castle[3] in 1975 and Ohkubo *et al.*[4] in 1990. The reduction of the slope of the line plotted by the ozone/current relationship as the temperature is increased was found for a concentric geometry, a wire plate geometry, and through this research a wire plane screen geometry. This research agreed with the conclusion of Ohkubo *et al.*[4] that the reduction of ozone production occurred with increased heating of the wire surface up to a limiting value. The limiting value found in Ohkubo *et al.*'s[4] work with positive corona was estimated to

be 100°C. As can be seen in Figures 12-14 in the Results section, the limiting value was found to be 85°C in this research with negative corona.

Although the general trend found in this research agreed with the work done in this field earlier, the degree of ozone reduction achieved by external wire heating varied. The work of Awad and Castle[3] reported, for a negative corona using a 0.028 inch (in.) Nichrome wire, a maximum reduction of 69% using external wire heating estimated to be 100°C. The work of Ohkubo *et al.*[4] reported for a negative corona setup (wire size and type not given) a 60% reduction while applying 0.44 W/cm (approximately 100°C) to the corona wire. This present research found a maximum ozone reduction of 48% with a Nichrome wire of 0.1 mm diameter at 84°C (0.43 W/cm), 53% with a Nichrome wire of 0.2 mm diameter at 84°C (0.45 W/cm), and 44% with a Nichrome wire of 0.3 mm diameter at 89°C (0.54 W/cm) as seen in Table 7. All the percentages in Table 7 were calculated on the basis of the maximum current that could be produced resulting in an ozone concentration of 50 ppb for a given set of conditions. The equations used to obtain the current values, found in a tabular form in the results section (Table 3), were the slopes of the lines of Figures 15-19 also found in the results section.

Awad and Castle[3] plotted ozone concentration versus corona current as a function of wire heating for nine wire materials. For Nichrome, a 70% ozone reduction resulted from

Table 7. Percent Reduction of Ozone Concentration due to external heating

Wire size (mm)	Temperature (°C)	Corona Current	Ozone	% Reduction
0.1	*	31.5	97	0
	38	31.5	85.2	12
	65	31.5	64.0	34
	84	31.5	50	48
	99	31.5	50	48
0.2	*	22.7	106.5	0
	43	22.7	87.7	18
	66	22.7	69.9	34
	84	22.7	50	53
	106	22.7	53	50
0.32	*	15.8	89.9	0
	49	15.8	86.1	4
	73	15.8	61.7	31
	89	15.8	50	44
	103	15.8	53.6	40

* - Room Temperature (No Wire Heating)

adding external wire heating estimated to be 100° C. Also, the slopes of their data when converted to ppb/μA were lower than those found in this study. The lower slopes are attributed to the variation in geometry between this present research and that of Awad and Castle[3], as discussed earlier in respect to ozone production as a function of wire size. Further, the reduction was attributed to the higher flow rate (5.66 L/s) used in their study compared to the 3.3 L/s flow rate studied here. The higher flow rate caused a dilution of the ozone concentration. A comparison of the two studies is presented in Table 8.

Accuracy of data

The data collection was carried out in as meticulously a manner as possible. However, due to the erratic nature of

Table 8. Slope Comparison between data collected by Awad and Castle[3] and the present study

WIRE			Slope
Type	Size (mm)	Temperature (°C)	(ppb/μA)
Nichrome[3]	0.7	*	5
		59	4
		79	2
		100	1.5
Nichrome	0.32	*	5.7
		49	5.5
		73	4.0
		89	3.2
		103	3.5

* - Room Temperature (No Wire Heating)

a corona discharge some error was inherent. The individual ozone concentration readings are believed to be within ± 2 ppb, the sensitivity experienced with the ozone monitor. The wire temperatures were calculated and are believed to be within ± 5°C, since the equations used in the computer program are theoretical and radiation and other losses are not accounted for in the program. A more accurate way of reporting the wire surface temperature is the use of the heating power applied to the electrode, since this was measured directly. However, temperatures were primarily used in this research because the temperatures convey more intuitive information. The power values corresponding to the temperatures reported are given in Table 9 so that the results of this research can be reproduced more accurately.

The average corona current was the most difficult measurement due to the fact that the higher the potential the

Table 9. Wire Surface Temperatures

Wire Diameter (m)	Wire Length (m)		Heating Power (W)		Wire Surface (°C)
	Total	Exposed*	Total	Corrected	
0.0001	0.64	0.42	5.4	3.5	38.2
			16.8	11.0	64.6
			28.0	18.4	84.1
			39.4	25.9	99.3
0.0002	0.635	0.42	7.3	4.8	43.4
			17.3	11.4	65.5
			28.2	18.9	84.0
			47.8	31.6	105.5
0.00032	0.67	0.42	11.2	7.0	48.8
			24.1	15.1	72.5
			36.2	22.7	89.0
			46.1	28.9	103.0

* - unexposed wire was inside capillary glass support tubing

more variable the corona current as illustrated in Figure 20. The current fluctuated by as much as ± 13 μA. The corona current variations were also due to the fact that the voltage supply was not regulated. Therefore, fluctuations in the voltage induced current fluctuations. Of course, these current fluctuations directly affected the ozone concentration. Therefore, the more unstable the corona the higher the standard deviation that was calculated for a group of ten ozone concentration readings. Even with these complications, the results obtained are believed to be valid because of the linear relationship obtained between the corona current and ozone concentration.

The humidity level was not controlled during this

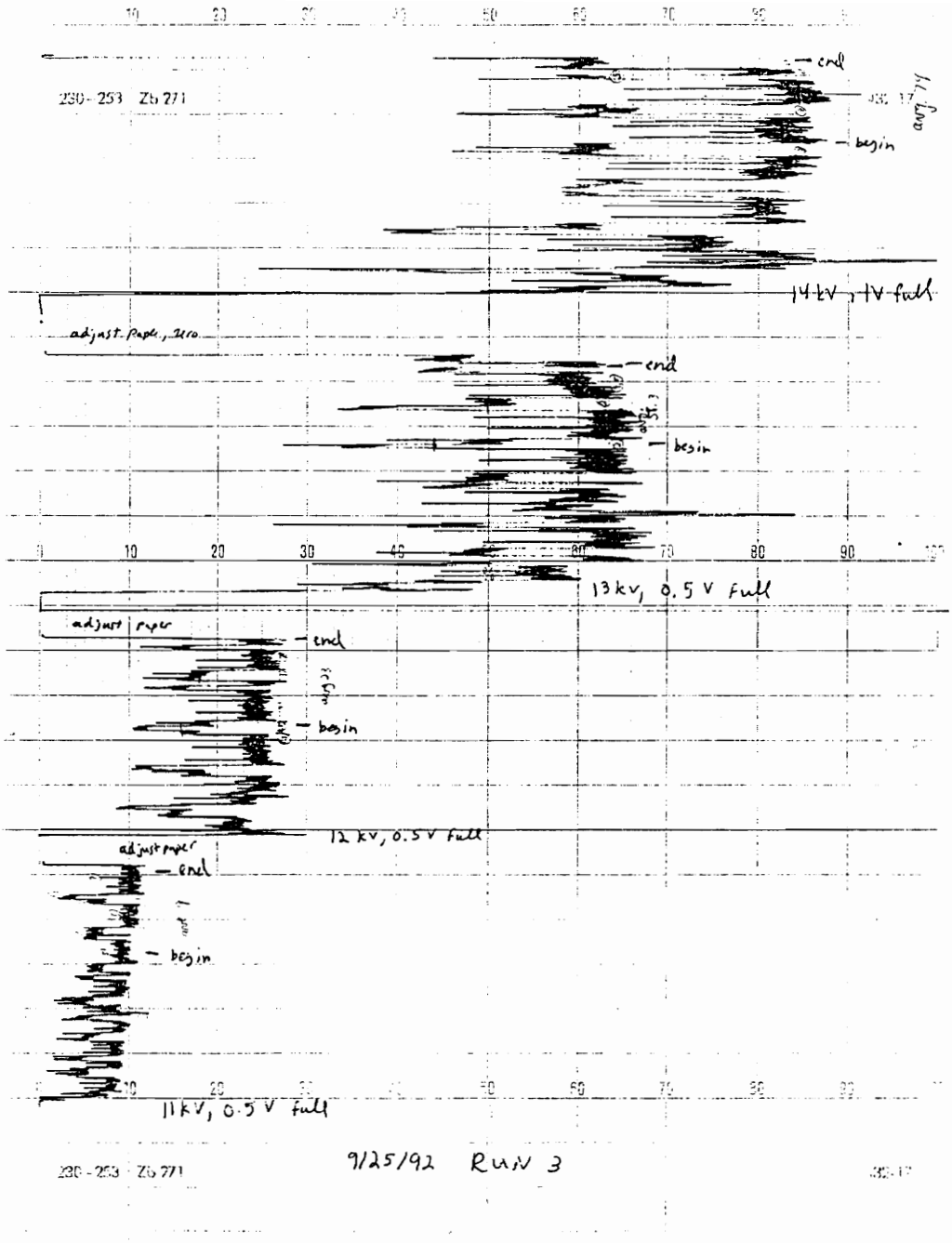

Figure 20. Strip Chart Recording for Corona Current

experimentation. However, even if the humidity were controlled only a slight increase or decrease in the ozone concentration would be expected. The humidity/ozone relationships reported in the literature were inconsistent. The goal of this research was to begin to develop a more effective air cleaner for the home or office. Humidity levels fluctuate indoors depending on such factors as the season (are windows open), the presence/absence of a humidifier, and the design of the HVAC system. Therefore, to rely on water vapor present in the air to counteract ozone production was not an effective solution. The approach of this research was that variations in humidity were a given and that the water vapor most likely would help lower ozone concentrations and at the worst raise concentrations by less than 1 percent.

Selection of best operating conditions

The factors that were important in achieving ideal operating conditions were (1) a high corona current, (2) generation of ozone concentrations below 50 ppb, and (3) wire strength. As discussed previously, the highest corona current levels were seen when external wire heating was added. Ozone generation rates decreased with external wire heating until the wire surface temperature was 85°C after which no further decrease was observed. Because of these facts, a wire surface temperature of at least 85°C was needed. As wire size decreased, an increase in corona

current was observed and the ozone generation rate decreased. Due to these observations, the smallest diameter wire (0.1 mm) was best. The question that remained was what would be the smallest wire diameter that would have sufficient strength. The strength of the wire refers to thermal strength because the wire elongated when exposed to high temperature and during arcing extremely high local heating caused the wire to melt. During the experimentation with the 0.1 mm wire, fracture occurred on two occasions. Both incidences occurred at the point of corona breakdown or arcing. Therefore if the required voltage potential to produce the desired corona current was close to the breakdown voltage potential, the 0.1 mm wire electrode size should not be used.

An essential criteria to meet was the 50 ppb ozone concentration limit set by the FDA. The highest current level of 31.5 μA occurred with the 0.1 mm wire operating at a surface temperature of 85^{o}C, using the slopes of the lines of Figures 15-19 and 50 ppb as the dependent variable. The negative voltage potential required in order to produce this current level was slightly above 10 kV. Since this voltage potential was 2000 V below the breakdown voltage, the use of the 0.1 mm wire was warranted. Ideal operating conditions for the wire-screen geometry studied seem to occur with the use of a 0.1 mm Nichrome wire with a negative potential of 10 kV and applied external wire heating power of 44 W/m which

corresponds to a wire surface temperature of 85°C (using computer program found in Appendix C). These operating conditions lead to a corona current of 30 μA with ozone concentration levels less than 50 ppb.

Recommendations

This research indicated that the indoor air cleaner model investigated was an attractive option for commercial development. Since no other air cleaner on the market at this point in time utilizes electrode wire heating, use of this approach should produce a more efficient type of cleaner. By using external wire heating the corona current was increased by nearly a factor of two and the ozone production was maintained at half the rate that would be expected for this amount of current. Therefore, there are more electrons available to ionize the air and the larger number of ionized gas atoms can collect more particulate matter.

Additional steps should be taken before a prototype is built. The first step is to size a fan to obtain a higher flow rate through the test section. Along with the fan size, the ideal cross section and length of the prototype need to be determined. These dimensions would be dependent upon the degree of portability of the indoor air cleaner (i.e. is it designed for tableside use or is it to be mounted to the ceiling). Obviously, a high flow rate though the test section is desired because this will decrease the ozone

concentrations; however, the flow has a limiting value because of particle reentrainment problems. The second step is to investigate the relationship between filter density and collection efficiency. This relationship would lead to the best choice of filter material. The third step is to experiment with even smaller electrode diameters (American gage sizes 39 and 40), since smaller wire diameters lead to the production of more corona current and lower ozone generation rates. The last step is to experiment with different geometries. It may be possible for a geometry to be developed in which there is a longer residence time in the vicinity of the electrode wire, similiar to that of the concentric wire-plate ESP design, which would lead to lower ozone production rates.

VI. Conclusions

The conclusions reached from the research performed using a negative corona discharge with external electrode wire heating are summarized as follows:

- The relationship between the corona current and voltage was parabolic and higher voltages produced higher current levels. A smaller wire diameter resulted in a lower onset voltage and higher corona currents overall. External wire heating permitted increased corona current for a given voltage.
- A linear relationship between corona current and ozone production existed. A smaller wire diameter lead to less ozone production for a given corona current. External wire heating lowered ozone concentrations, but did not further reduce ozone concentrations for calculated electrode wire temperatures exceeding 85°C.
- With the highest beneficial amount of external wire heating, an increase of 110% in corona current could be achieved and a 52% reduction in ozone concentration could also be accomplished.
- A 0.1 mm wire operated at a negative potential of 10 kV produced a corona current of approximately 30 μA and generated less than 50 ppb ozone, the FDA standard.

VII. References

1. Godish, T. (1989). *Indoor Air Pollution Control*. Lewis Publishers, Inc., Chelsea, MI, 401 p.

2. "Code of Federal Regulations," Title 21, Part 801.415, U.S. Government Printing Office, Washington, D.C., April 1992.

3. Awad, M.B. and Castle, G.S.P., "Ozone Generation in an Electrostatic Precipitator With a Heated Corona Wire." *Journal of the Air Pollution Control Association*, *25*, 4, 369-374 (1975).

4. Ohkubo, T., Hamasaki, S., Nomoto, Y., Chang, J.S., and Adachi, T. "Effect of Corona Wire Heating on the Downstream Ozone Concentration Profiles in an Air-cleaning Wire-duct Electrostatic Precipitator." *IEEE Transactions On Industry Applications.*, *26*, 3, 542-549 (1990).

5. Castle, G.S.P., Inculet, I.I. and Burgess, K.I. "Ozone Generation in Positive Corona Electrostatic Precipitators." *IEEE Transactions On Industry And General Applications*, IGA-5, 4, 489-496 (1969).

6. Loeb, L.B. (1965). *Electrical Coronas Their Basic Physical Mechanisms*. University of California Press, Berkeley and Los Angles, CA, 694 p.

7. Rose, H.E. and Wood, A.J. (1966) *An Introduction to Electrostatic Precipitation in Theory and Practice*. Constable and Company Ltd., London, 212 p.

8. White, H.J. (1963). *Industrial Electrostatic Precipitation*. Addison-Wesley Publishing Company, Inc., Reading, MA, 376 p.

9. Rice, R.G. and Netzer, A. (1982). *Handbook Of Ozone Technology And Applications*, Vol. 1, Ann Arbor Science Publishers, Ann Arbor, MI.

10. Viner, S., Lawless, P.A., Ensor, D.S., and Sparks, L.E. (1989). Ozone Generation In D.C.-Energized Electrostatic Precipitators. *Conference Record*, IAS Annual Meeting (IEEE Industry Applications Society) Part II, Oct. 1-5, 1989, 2167-2174.

11.Amouroux, J. and Goldman A. (1983). Plasma Chemistry. in: *Electrical Breakdown and Discharge in Gases. Part B, Macroscopic Processes and Discharges*, E. E. Kunhardt and L. H. Luessen, eds., Plenum Press, New York, NY, 293-346.

12.Offermann, F.J., Sextro, R.G., Fisk, W.J., Grimsrud, D.T., Nazaroff, W.W., Nero, A.V., Revzan, K.L., and Yater, J. "Control of Respirable Particles In Indoor Air With Portable Air Cleaners." *Atmospheric Environment, 19*, 11, 1761-1771 (1985).

13.Jokl, M.V. (1989). *Microenvironment : The Theory and Practice of Indoor Climate*. Charles C. Thomas, Springfield, IL, 416 p.

14.Osborn, P.D. (1989). *The Engineer's Clean Air Handbook*. Butterworth & Co. Ltd., London, 201 p.

15.Morgan, V. T. "The thermal rating of overhead-line conductors, Part I: The steady-state thermal model." *Elec. Power Syst. Res., 5*, 119-139 (1982).

16.Chang, J. S. and Laframboise, G. "Conductive heat transfer to an arbitrarily shaped body in a variable property fluid." *Int. J. Heat Mass Transfer, 21*, 360-362 (1978).

VIII. APPENDIX A - Data Tables

Table 10. Data Collection Performed on 9/24/92 RUN #2

Flow	Voltage Potential	Corona Current	Heating Power	Ozone Production (ppb)												Ion Current
cfm	kV	μA	W	1	2	3	4	5	6	7	8	9	10	AVG	std dev	μA
7.0	---	---	---	21	22	24	26	15	18	22	19	18	14	19.9	3.62	---
7.0	8.5	2.1	5.4	22	29	27	22	22	21	26	22	24	28	24.3	2.79	---
7.0	10	10.9	5.4	53	37	48	43	49	42	49	43	49	50	46.3	4.58	0.2
7.0	11	20.6	5.4	78	67	76	67	74	72	82	65	68	71	72.0	5.22	0.5
7.1	12	41.6	5.4	133	125	142	142	130	138	136	126	124	121	131.7	7.25	1.0
7.1	13	79.1	5.4	244	238	241	182	215	245	237	241	241	237	232.1	18.5	2.0

Wire Diameter = 0.1 mm Sampling Flow Rate = 2 LPM
Screen Spacing = 8 cm Ground Spacing = 2 cm Sampling Spacing = 25 cm
NOTE : All spacing distances in reference to corona wire

Ion Screen Potential = 100 V
Temperature = 21 ^{o}C Bar. Pressure = 718 mm Hg Humidity = 52% R.H.

Table 11. Data Collection Performed on 9/24/92 RUN #3

Flow	Voltage Potential	Corona Current	Heating Power	Ozone Production (ppb)												Ion Current
cfm	kV	μA	W	1	2	3	4	5	6	7	8	9	10	AVG	std dev	μA
7.1	---	---	16.8	23	25	25	21	22	20	24	25	20	25	23.0	2.0	---
7.1	8.0	1.5	16.8	25	24	28	22	27	25	26	28	21	20	24.6	2.7	---
7.1	9.0	2.7	16.8	25	31	31	28	33	27	29	29	31	30	29.4	2.2	0.1
7.1	10	15.8	16.8	57	54	51	47	55	52	46	52	56	58	52.8	3.8	0.5
7.1	11	27.5	16.8	82	69	68	83	84	72	80	83	68	62	75.1	7.7	1.0
7.1	12	49.5	16.8	117	119	120	117	118	119	117	122	112	117	118	2.5	1.5
7.1	13	100.	16.8	233	234	235	227	228	230	227	226	228	224	229	3.5	2.0

Wire Diameter = 0.1 mm Sampling Flow Rate = 2 LPM
Screen Spacing = 8 cm Ground Spacing = 2 cm Sampling Spacing = 25 cm
NOTE : All spacing distances in reference to corona wire

Ion Screen Potential = 100 V
Temperature = 22 °C Bar. Pressure = 718 mm Hg Humidity = 59% R.H.

Table 12. Data Collection Performed on 9/24/92 RUN #4

Flow	Voltage Potential	Corona Current	Heating Power	Ozone Production (ppb)												Ion Current
cfm	kV	μA	W	1	2	3	4	5	6	7	8	9	10	AVG	std dev	μA
7.1	---	---	28.0	22	25	29	23	26	26	25	29	28	25	25.8	2.2	---
7.1	6.0	0.5	28.0	23	25	26	28	26	26	27	23	29	23	25.6	2.0	---
7.1	8.0	8.5	28.0	44	38	39	36	35	36	38	41	37	33	37.7	3.0	0.2
7.1	9.0	15.0	28.0	49	47	45	49	48	41	42	43	51	41	45.6	3.5	0.8
7.1	10	29.9	28.0	60	65	62	71	68	63	70	71	64	68	66.2	3.7	1.0
7.1	11	47.1	28.0	100	96	94	94	97	86	110	100	104	106	98.7	6.5	1.8
7.1	12	80.3	28.0	163	159	161	137	163	161	159	167	164	161	160	7.8	2.0

Wire Diameter = 0.1 mm Sampling Flow Rate = 2 LPM
Screen Spacing = 8 cm Ground Spacing = 2 cm Sampling Spacing = 25 cm
NOTE : All spacing distances in reference to corona wire

Ion Screen Potential = 100 V
Temperature = 22.7 °C Bar. Pressure = 718 mm Hg Humidity = 69% R.H.

Table 13. Data Collection Performed on 9/24/92 RUN #5

Flow	Voltage Potential	Corona Current	Heating Power	Ozone Production (ppb)												Ion Current
cfm	kV	μA	W	1	2	3	4	5	6	7	8	9	10	AVG	std dev	μA
7.1	---	---	39.4	24	26	22	22	25	28	29	30	25	23	25.4	2.69	---
7.1	6.0	0.25	39.4	24	26	27	26	28	33	25	27	25	26	26.7	2.37	---
7.1	8.0	12.7	39.4	46	43	36	45	42	45	44	40	50	45	43.6	3.56	0.3
7.1	9.0	22.1	39.4	57	54	55	56	51	55	53	52	59	57	54.9	2.34	0.8
7.1	10	40.9	39.4	81	83	87	85	82	87	84	82	81	67	81.9	5.39	1.5
7.1	11	71.0	39.4	141	144	142	118	135	139	135	135	138	148	138	7.66	2.0
7.1	12	128.	39.4	211	262	255	257	258	262	199	203	272	257	244	26.2	2.2

Wire Diameter = 0.1 mm Sampling Flow Rate = 2 LPM
Screen Spacing = 8 cm Ground Spacing = 2 cm Sampling Spacing = 25 cm
NOTE : All spacing distances in reference to corona wire

Ion Screen Potential = 100 V
Temperature = 22 ^{o}C Bar. Pressure = 718 mm Hg Humidity = 61% R.H.

Table 14. Data Collection Performed on 9/25/92 RUN #1

Flow	Voltage Potential	Corona Current	Heating Power	Ozone Production (ppb)												Ion Current
cfm	kV	μA	W	1	2	3	4	5	6	7	8	9	10	AVG	std dev	μA
7.1	---	---	---	14	20	18	19	20	16	16	17	21	20	18.1	2.17	---
7.1	12	1.5	---	29	14	24	26	23	21	28	28	24	23	24.0	4.15	---
7.1	13	5.4	---	40	33	46	46	38	40	48	44	45	34	41.4	4.96	0.1
7.1	14	11.0	---	66	69	65	78	67	56	56	71	78	77	68.3	7.69	0.5
7.1	15	25.5	---	153	147	143	149	104	112	114	150	148	137	135.7	17.5	1.0

Wire Diameter = 0.2 mm Sampling Flow Rate = 2 LPM
Screen Spacing = 8 cm Ground Spacing = 2 cm Sampling Spacing = 25 cm
NOTE : All spacing distances in reference to corona wire

Ion Screen Potential = 100 V
Temperature = 20 °C Bar. Pressure = 717 mm Hg Humidity = 62% R.H.

Table 15. Data Collection Performed on 9/25/92 RUN #2

Flow	Voltage Potential	Corona Current	Heating Power	Ozone Production (ppb)												Ion Current
cfm	kV	μA	W	1	2	3	4	5	6	7	8	9	10	AVG	std dev	μA
7.1	---	---	7.3	19	14	9	20	16	21	14	18	17	16	16.4	3.32	---
7.1	12	4.7	7.3	30	26	36	34	35	39	35	33	35	27	33.0	3.90	---
7.1	13	11.3	7.3	70	48	57	69	74	62	55	43	56	69	60.3	9.72	0.2
7.1	14	31.4	7.3	149	114	147	108	146	143	147	110	141	147	135.2	16.3	0.8

Wire Diameter = 0.2 mm Sampling Flow Rate = 2 LPM
Screen Spacing = 8 cm Ground Spacing = 2 cm Sampling Spacing = 25 cm
NOTE : All spacing distances in reference to corona wire

Ion Screen Potential = 100 V
Temperature = 22 ^{o}C Bar. Pressure = 717 mm Hg Humidity = 65% R.H.

Table 16. Data Collection Performed on 9/25/92 RUN #3

Flow	Voltage Potential	Corona Current	Heating Power	Ozone Production (ppb)												Ion Current
cfm	kV	μA	W	1	2	3	4	5	6	7	8	9	10	AVG	std dev	μA
7.1	---	---	17.3	22	18	15	21	20	14	16	17	15	12	17.0	3.1	---
7.1	11	4.4	17.3	31	29	27	26	32	34	25	26	32	30	29.2	2.9	---
7.1	12	11.3	17.3	34	53	46	54	40	47	49	51	55	53	48.2	6.4	0.3
7.1	13	28.6	17.3	67	105	108	107	77	91	107	101	103	104	97.0	14	1.0
7.1	14	72.5	17.3	198	260	262	259	217	276	270	269	259	196	246.6	29	1.8

Wire Diameter = 0.2 mm Sampling Flow Rate = 2 LPM
Screen Spacing = 8 cm Ground Spacing = 2 cm Sampling Spacing = 25 cm
NOTE : All spacing distances in reference to corona wire

Ion Screen Potential = 100 V
Temperature = 23 °C Bar. Pressure = 717 mm Hg Humidity = 60% R.H.

Table 17. Data Collection Performed on 9/25/92 RUN #4

Flow	Voltage Potential	Corona Current	Heating Power	Ozone Production (ppb)												Ion Current
cfm	kV	μA	W	1	2	3	4	5	6	7	8	9	10	AVG	std dev	μA
7.1	---	---	28.2	20	20	30	22	19	23	25	18	21	24	22.2	3.3	---
7.1	10	2.7	28.2	28	24	26	21	27	23	28	25	27	28	25.7	2.3	---
7.1	11	8.4	28.2	40	30	36	40	32	38	38	40	27	41	36.2	4.6	0.3
7.1	12	18.9	28.2	62	64	64	48	53	63	61	59	66	67	60.7	5.7	0.8
7.1	13	34.3	28.2	89	101	100	95	102	103	103	79	103	107	98.2	8.0	1.0
7.1	14	90.7	28.2	239	248	177	249	202	238	247	248	195	236	227.9	25	1.8

Wire Diameter = 0.2 mm Sampling Flow Rate = 2 LPM
Screen Spacing = 8 cm Ground Spacing = 2 cm Sampling Spacing = 25 cm
NOTE : All spacing distances in reference to corona wire

Ion Screen Potential = 100 V
Temperature = 23 °C Bar. Pressure = 717 mm Hg Humidity = 62% R.H.

Table 18. Data Collection Performed on 9/25/92 RUN #5

Flow	Voltage Potential	Corona Current	Heating Power	Ozone Production (ppb)												Ion Current
cfm	kV	μA	W	1	2	3	4	5	6	7	8	9	10	AVG	std dev	μA
7.1	---	---	47.8	17	16	15	16	21	19	18	18	19	25	18.4	2.8	---
7.1	10	5.4	47.8	29	29	31	28	33	28	31	31	25	30	29.5	2.1	0.2
7.1	11	14.7	47.8	55	46	54	50	36	54	54	54	54	42	49.9	6.2	0.3
7.1	12	24.5	47.8	72	74	69	75	80	78	60	75	59	81	72.3	7.2	1.0
7.1	13	61.3	47.8	181	172	116	171	168	171	180	178	161	140	163.8	20	1.8

Wire Diameter = 0.2 mm Sampling Flow Rate = 2 LPM
Screen Spacing = 8 cm Ground Spacing = 2 cm Sampling Spacing = 25 cm
NOTE : All spacing distances in reference to corona wire

Ion Screen Potential = 100 V
Temperature = 21 °C Bar. Pressure = 717 mm Hg Humidity = 68% R.H.

Table 19. Data Collection Performed on 10/5/92 RUN #1

Flow	Voltage Potential	Corona Current	Heating Power	Ozone Production (ppb)												Ion Current
cfm	kV	μA	W	1	2	3	4	5	6	7	8	9	10	AVG	std dev	μA
7.0	---	---	---	19	19	20	19	24	21	22	19	18	18	19.9	1.8	---
7.0	14.5	1.0	---	24	25	15	22	26	23	30	27	28	27	24.7	4.0	---
7.0	15	1.4	---	32	28	28	33	25	25	24	24	24	19	26.2	3.9	0.5
7.0	16	15.4	---	114	117	117	125	115	67	98	104	99	103	106	16	0.8

Wire Diameter = 0.32 mm Sampling Flow Rate = 2 LPM
Screen Spacing = 8 cm Ground Spacing = 2 cm Sampling Spacing = 25 cm
NOTE : All spacing distances in reference to corona wire

Ion Screen Potential = 100 V
Temperature = 20.8 °C Bar. Pressure = 714.3 mm Hg Humidity = 47% R.H.

Table 20. Data Collection Performed on 10/5/92 RUN #2

Flow	Voltage Potential	Corona Current	Heating Power	Ozone Production (ppb)												Ion Current
cfm	kV	μA	W	1	2	3	4	5	6	7	8	9	10	AVG	std dev	μA
7.0	---	---	11.2	24	19	24	23	17	20	20	22	20	17	20.6	2.5	---
7.0	14	5.5	11.2	44	46	48	49	48	45	55	48	51	48	48.2	3.0	---
7.0	15	20.2	11.2	112	114	124	129	132	134	135	137	137	138	129.2	9.0	0.5

Wire Diameter = 0.32 mm Sampling Flow Rate = 2 LPM
Screen Spacing = 8 cm Ground Spacing = 2 cm Sampling Spacing = 25 cm
NOTE : All spacing distances in reference to corona wire

Ion Screen Potential = 100 V
Temperature = 21 °C Bar. Pressure = 714 mm Hg Humidity = 46% R.H.

Table 21. Data Collection Performed on 10/5/92 RUN #3

Flow	Voltage Potential	Corona Current	Heating Power	Ozone Production (ppb)												Ion Current
cfm	kV	μA	W	1	2	3	4	5	6	7	8	9	10	AVG	std dev	μA
7.0	---	---	24.1	18	24	24	20	20	21	19	20	26	23	21.5	2.5	---
7.0	13	3.0	24.1	30	32	37	19	27	24	34	21	35	32	29.1	5.8	0.1
7.0	14	12.9	24.1	52	55	83	64	86	85	60	51	87	88	71.1	15	0.5

Wire Diameter = 0.32 mm Sampling Flow Rate = 2 LPM
Screen Spacing = 8 cm Ground Spacing = 2 cm Sampling Spacing = 25 cm
NOTE : All spacing distances in reference to corona wire

Ion Screen Potential = 100 V
Temperature = 22 °C Bar. Pressure = 714 mm Hg Humidity = 44% R.H.

Table 22. Data Collection Performed on 10/5/92 RUN #4

Flow	Voltage Potential	Corona Current	Heating Power	Ozone Production (ppb)												Ion Current
cfm	kV	μA	W	1	2	3	4	5	6	7	8	9	10	AVG	std dev	μA
7.0	---	---	36.2	18	22	13	19	20	20	18	18	22	22	19.2	2.6	---
7.0	12	4.1	36.2	35	31	33	29	34	31	28	33	37	30	32.1	2.7	---
7.0	13	8.7	36.2	55	34	50	49	47	42	35	47	49	55	46.3	6.9	0.5

Wire Diameter = 0.32 mm Sampling Flow Rate = 2 LPM
Screen Spacing = 8 cm Ground Spacing = 2 cm Sampling Spacing = 25 cm
NOTE : All spacing distances in reference to corona wire

Ion Screen Potential = 100 V
Temperature = 22 °C Bar. Pressure = 714 mm Hg Humidity = 42% R.H.

Table 23. Data Collection Performed on 10/5/92 RUN #5

Flow	Voltage Potential	Corona Current	Heating Power	Ozone Production (ppb)												Ion Current
cfm	kV	μA	W	1	2	3	4	5	6	7	8	9	10	AVG	std dev	μA
7.0	---	---	46.1	15	21	14	20	17	21	17	21	23	22	19.1	3.0	---
7.0	12	4.3	46.1	20	34	39	20	36	33	29	35	29	30	30.5	6.1	---
7.0	13	15.7	46.1	49	86	82	74	81	55	57	85	90	60	71.9	14.	0.5

Wire Diameter = 0.32 mm Sampling Flow Rate = 2 LPM
Screen Spacing = 8 cm Ground Spacing = 2 cm Sampling Spacing = 25 cm
NOTE : All spacing distances in reference to corona wire

Ion Screen Potential = 100 V
Temperature = 22.8 °C Bar. Pressure = 714 mm Hg Humidity = 41% R.H.

Table 24. Corrected Ozone Concentrations

Wire Size (m)	Run #1		RUN #2		RUN #3		RUN #4		RUN #5	
	$O_{3\ meas.}$	$O_{3\ act.}$	$O_{3\ meas.}$	$O_{3\ act.}$	$O_{3\ meas.}$	$O_{3\ act.}$	$O_{3\ meas.}$	$O_{3\ act.}$	$O_{3\ meas}$	$O_{3\ act.}$
0.0001	20.9	19.0	19.9	18.0	23.0	21.1	25.8	24.0	25.4	23.6
	21.5	19.6	24.3	22.5	24.6	22.8	25.6	23.8	26.7	24.9
	26.2	24.4	46.3	44.9	29.4	27.7	37.7	36.1	43.6	42.1
	45.1	43.7	72.0	71.1	52.8	51.5	45.6	44.2	54.9	53.7
	85.2	84.6	131.7	132.0	75.1	74.3	66.2	65.2	81.9	81.2
	203.7	205.4	232.1	234.4	117.8	117.8	98.7	98.3	137.5	137.9
	---	---	---	---	229.2	231.5	159.5	160.4	243.6	246.1
0.0002	18.1	16.1	16.4	14.4	17.0	15.0	22.2	20.3	18.4	16.4
	24.0	22.2	33.0	31.3	29.2	27.5	25.7	23.9	29.5	27.8
	41.4	39.9	60.3	59.2	48.2	46.8	36.2	34.6	49.9	48.6
	68.3	67.3	135.2	135.6	97.0	96.6	60.7	59.6	72.3	71.4
	135.7	136.1	---	---	246.6	249.2	98.2	97.8	163.8	164.7
	---	---	---	---	---	---	227.9	230.1	---	---
0.00032	19.9	18.0	20.6	18.7	21.5	19.6	19.2	17.3	19.1	17.2
	24.7	22.9	48.2	46.8	29.1	27.4	32.1	30.4	30.5	28.8
	26.2	24.4	129.2	129.5	71.1	70.2	46.3	44.9	71.9	71.0
	105.9	105.7	---	---	---	---	---	---	---	---

IX. APPENDIX B - Calibration Procedure

Table 25. Data for Sharp Edge Orifice Calibration

Manometer (Inches of Water)	Flow (cfm)
2.0	26.25
1.5	21.25
1.0	18.125
0.5	12.5
0.25	9.375
0.2	7.75
0.15	6.75
0.1	5.5
0.05	3.875

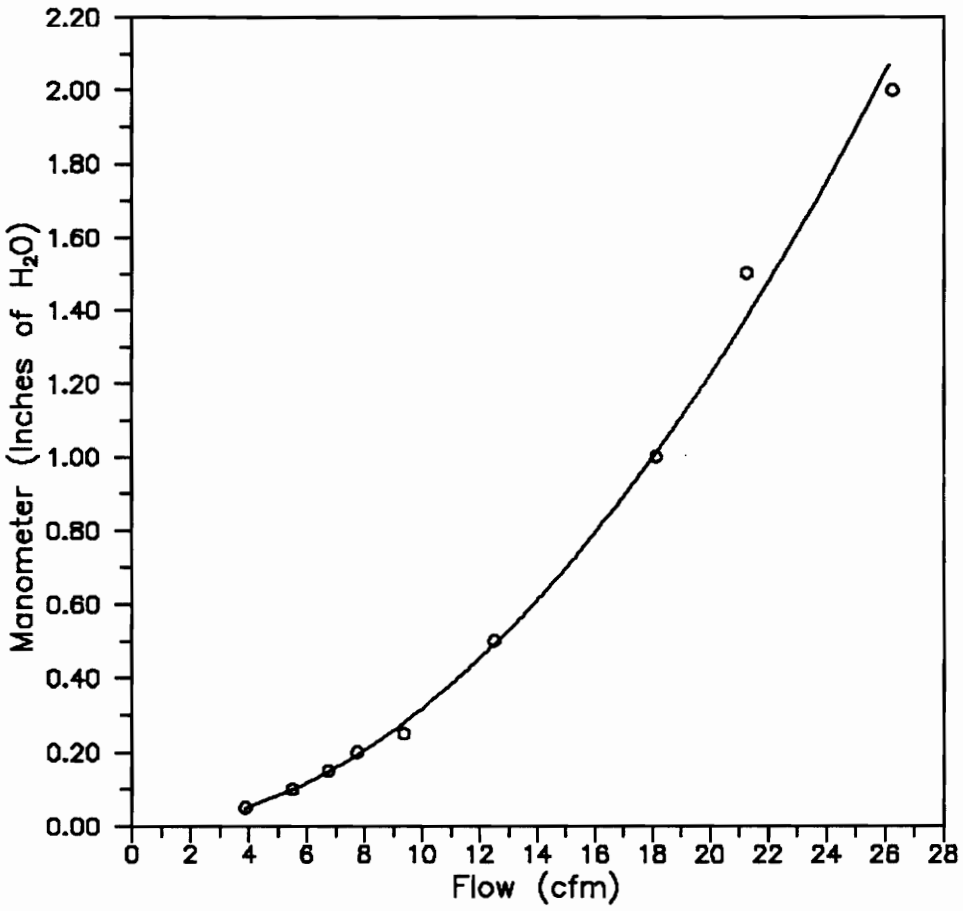

Figure 21. Calibration Curve for Sharp Edge Orifice

Ozone Monitor Calibration

The ozone monitor calibration was performed in the following manner. The Dasibi 1003-RS monitor was compared to a calibration standard. The standard was produced by a CSI Photocal 3000 which had been calibrated by the EPA. The source used as the input for this device was dry bottled air. The ozone generator was turned on and allowed to run for the recommended time of 20 minutes. The generator was set on 400 ppb and eight reading were taken from the generator display and the ozone monitor display. At the end of the eight readings the readings for both devices were averaged. Then the average for the generator was corrected by 0.985 a correction found by the calibration with the EPA machine. This procedure was then repeated for 300, 150 and 0 ppb. From the average values, the calibration curve was plotted.

Table 26. Data for Dasibi Ozone Monitor Calibration

Reading	Run #1		Run #2		Run #3		Run #4	
	Ozone Generated (ppb)	Ozone Measured (ppb)	Ozone Generated (ppb)	Ozone Measured (ppb)	Ozone Generated (ppb)	Ozone Measured (ppb)	Ozone Generated (ppb)	Ozone Measured (ppb)
1	408	413	299	306	160	158	4	4
2	408	406	299	303	157	144	0	4
3	407	403	300	305	154	146	1	5
4	404	405	298	304	144	146	2	6
5	403	404	297	303	149	149	2	7
6	404	400	297	304	150	151	1	3
7	402	396	299	306	148	148	0	6
8	401	405	300	307	150	151	0	6
Average	404.6	404	298.6	304.8	151.5	149.1	1.25	5.13
Actual	410.8	---	303.1	---	153.8	---	1.27	---

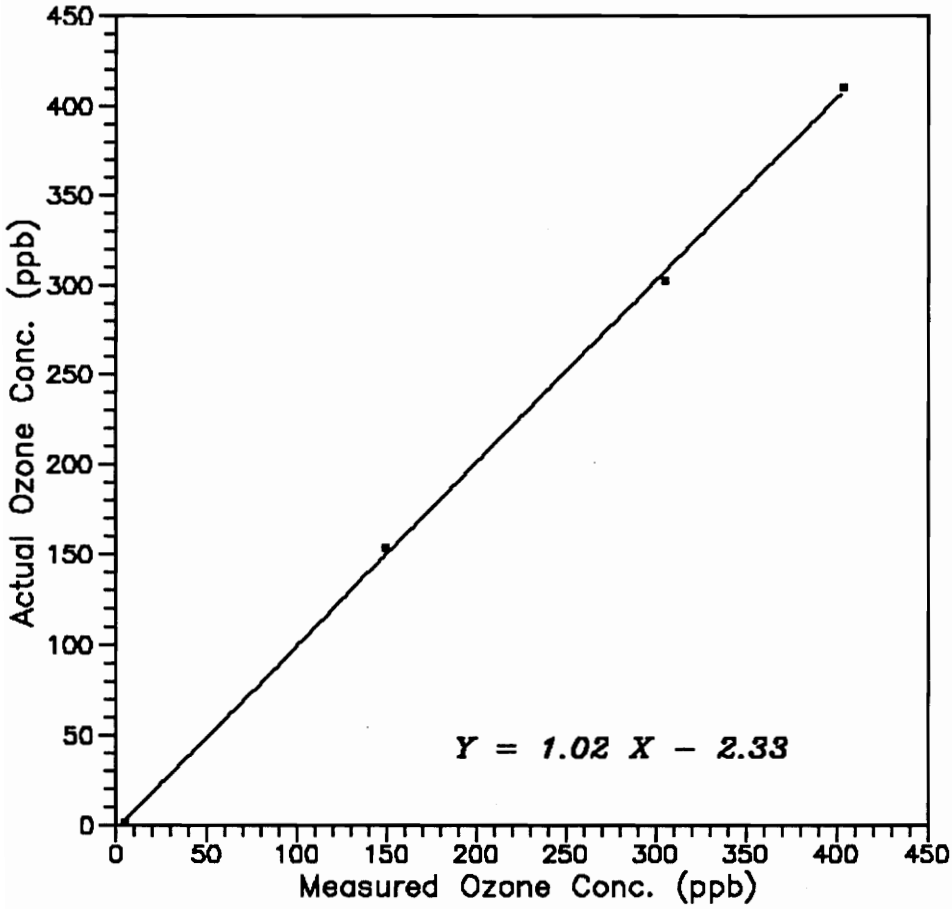

Figure 22. Calibration Curve for Dasibi Ozone Monitor

X. APPENDIX C - Computer program listing

```
      PROGRAM WIRE TEMPERATURE
      REAL PIN,LF,TW,TWO,TA,NUO,NU,TF,RE,TB
      REAL VG,NF,DIFF,D,L
      INTEGER  TYPE,CALC
*****************************************************************
DEFINITION OF VARIABLES

PIN- Power Input                    LF- Thermal Conductivity of
Fluid
TW - Temperature of Wire      TWO- Initial Wire Temperature
TA- Ambient Air Temperature   NUO- Initial Nusselt Number
NU- Modified Nusselt Number   TF- Film Temperature
RE- Reynolds Number           TB- Temperature ratio (TW/TA)
VG- Volume of Gas             NF- Velocity of fluid
DIFF- % difference            D- Diameter of wire
L- length of wire             TYPE - type of calculation
CALC- loop control variable
*****************************************************************
      OPEN(10,FILE='WT.OUT',STATUS='UNKNOWN')
      OPEN(20,FILE='WT.DAT',STATUS='UNKNOWN')
      CALC = 1
      WRITE(10,30)
      DO WHILE (CALC .EQ. 1)
       READ(20,*) TWO,TA,VG,D,L,TYPE,CALC
       DIFF = 100.0
       IF (TYPE .EQ. 1) THEN
           PRINT*,'POWER INPUT (W)'
           READ*,PIN
       ENDIF
       DO WHILE (DIFF .GT. 1)
*        Physical Properties of calculations                  *
*        Equations developed by Morgan[15]                    *
*        or Chang and Laframboise[16]                         *
         TF=(TWO+TA)/2.0
         NF=1.32E-5 + 9.5E-8*TF
         RE=(VG*D)/NF
         LF=2.42E-2 + 7.2E-5*TF
         TB=TWO/TA
         NUO=(1.12/ALOG(2.0))*((1.0-TB**1.78)/(1.0-TB))
         NU=NUO+0.795*RE**0.384
         IF (TYPE .EQ. 1) THEN
*          Calculation for Wire Surface Temperature      *
           TW=0.8*PIN/(3.14159*LF*NU*L) + TA
           DIFF=(ABS(TW-TWO)/TW)*100.0
         ELSE
*          Calculation for Power Input                   *
            PIN=3.14159*LF*(TWO-TA)*NU*L/0.8
            DIFF =1.0
         ENDIF
         IF (TYPE .EQ. 1) THEN
           TWO=TW
```

```
            ENDIF
          ENDDO
          WRITE(10,20)
          WRITE(10,40) D,L,TWO,PIN
          ENDDO
20      FORMAT('  ')
30      FORMAT('  DIAMETER (M)',1X,' LENGTH (M) ',2X,'SURFACE
',
     1 'TEMPERATURE (C)',2X,'POWER INPUT (W)')
40      FORMAT(' ',3X,E7.1,6X,E7.1,14X,F5.1,16X,F5.1)
        END
```

XI. Vita

The author was born in Richmond, Virginia on December 14, 1968. He would remain in Richmond until his college days. He graduated from Trinity Episcopal High School as Salutatorian in May 1987. He then attended Washington University in St. Louis for a year and a half and then transferred to Villanova University. He graduated, Magna cum Laude, from Villanova in 1991 with a Bachelor's degree in Mechanical Engineering. He then attended Graduate School at Virginia Polytechnic Institute and State University to pursue a Master's Degree in Environmental Engineering. At Virginia Tech, he met Dr. J. Martin Hughes and decided to specialize in Air Resources Engineering. He hopes to design Air Pollution Control Equipment in the future.